ImmunoTargets and Therapy

Dovepress
Taylor & Francis Group

Open Access Full Text Article

ORIGINAL RESEARCH

Conversion of T Effector Cells Into T Regulatory Cells in Type 1 Diabetes/Latent Autoimmune Diabetes of Adults by Inhibiting eIF5A and Notch Pathways

Shafiya Imtiaz Rafiqi[1,2], Ahmad Aldasouqi[1–3], Rodis D Paparodis[4,5], Sandesh Dewan[1,2], Aneeba Farooqi[1,2], Sarah Faisal[1,6], Yousuf Nemat[1,7], Nancy Salim[1,2], Salauddin Qureshi[1,8], Asif Mahmood[9], Yara Tovar[1,2], John Y Jun[1,2], Andrea L Kalinoski[10], Raghavendra G Mirmira[11], Juan Carlos Jaume[5], Shahnawaz Imam[1,2]

[1]Division of Endocrinology, Diabetes and Metabolism, Department of Medicine, College of Medicine and Life Sciences, University of Toledo, Toledo, OH, USA; [2]Center for Diabetes and Endocrine Research (CeDER), College of Medicine and Life Sciences, University of Toledo, Toledo, OH, USA; [3]College of Natural Sciences and Mathematics, University of Toledo, Toledo, OH, USA; [4]Hellenic Endocrine Network, Athens, Greece, Endocrinology, Diabetes and Metabolism Clinics, Private Practice, Patras, Greece; [5]Stritch School of Medicine/Edward Hines, Jr. VA Hospital, Loyola University Chicago, Hines, IL, USA; [6]College of Art and Science, Case Western Reserve University, Cleveland, OH, USA; [7]Florida Atlantic University, Boca Raton, FL, USA; [8]Division of Biological Standardization, ICAR-Indian Veterinary Research Institute, Izatnagar, Bareilly, India; [9]University of Toledo Medical Centre, Hospital Medicine, University of Toledo, Toledo, OH, USA; [10]Department of Surgery, Integrated Core Facilities, University of Toledo, Toledo, OH, USA; [11]Division of the Biological Sciences, the University of Chicago, Chicago, IL, USA

Correspondence: Shahnawaz Imam, Center for Diabetes and Endocrine Research (CeDER), College of Medicine and Life Sciences, BHS386, Mail Stop 3000 Arlington Ave. University of Toledo, Toledo, OH, 43614-2598, USA, Tel +1 419-383-3786, Email shahnawaz.imam@utoledo.edu

Background: The generation of functionally active, stable T regulatory cells (Tregs) is a crucial target of type 1 diabetes (T1D) immunotherapy. This study investigated therapeutic intervention for T1D/Latent autoimmune diabetes in adults (LADA), wherein the diabetogenic proinflammatory Treg (intermediate) cell subset was characterized and driven to a Treg phenotype ($CD4^+CD25^+FOXP3^+$). This involved simultaneous inhibition of the eukaryotic initiation factor 5a (eIF5a) and Notch pathways using GC7 (N1-Guanyl-1,7-diaminoheptane) and Anti-DLL4 (Delta-like-ligand-4).

Methods: Peripheral blood from patients with T1D/LADA and healthy adults (n=7 each) was used to isolate the $CD4^+CD25^-$ T cell population and CD4 deficient peripheral blood mononuclear cells (PBMCs). Cells were subjected to GAD65+GC7+anti-DLL4 treatment for seven days and compared with conventional anti-CD3/CD28/CD137 stimulation for conversion into the Tregs. Newly plasticized Tregs were assessed for their suppressive potential against freshly isolated autologous T responder cells. In addition, live, dead, and apoptotic cell counts were performed to evaluate the adverse effects of immunomodulatory treatment on immune cells. The data was analyzed with GraphPad Prism using 1- or 2-way ANOVA and a Student's *t*-test.

Results: A unique population of proinflammatory cytokines expressing intermediate Tregs ($CD4^+CD25^-IFNg^+IL17^+FOXP3^+$) was characterized in T1D/LADA patients and found significantly increased compared to age-matched healthy adults. Simultaneous inhibition of eIF5a and Notch pathways could induce Treg phenotype in Treg-deficient $CD4^+$ T cells and CD4 deficient PBMCs from T1D/LADA patients. GAD65+GC7+anti-DLL4 treatment plasticized Tregs withstanding a proinflammatory milieu mimicking T1D/LADA, and the plasticized Tregs exhibited a stable and suppressive functional phenotype. Furthermore, GAD65+GC7+anti-DLL4 treatment had no adverse effects on immune cells.

The present approach is a multipronged approach involving the inhibition of eIF5a and Notch pathways that addresses the upregulation of immune tolerance, differentiation, and proliferation of cytotoxic T cells and alleviates β-cell dysfunction. Additionally, this treatment strategy could also be leveraged to boost Treg generation following islet transplantation or as a combinational therapy along with adoptive cell transfer.

Keywords: autoimmune disorders, eIF5a, immunomodulation, immune cell plasticity, latent autoimmune diabetes in adults, notch, transdifferentiation, type 1 diabetes, unfit tregs

Received: 7 November 2024
Accepted: 22 February 2025
Published: 13 March 2025

Background

Immune cell plasticity is the ability of immune cells to switch between functional states in response to the cytokine milieu. A large body of literature supports the idea that T cells change their initial lineage commitment to different functional phenotypes in response to signals from the microenvironment, including cytokines, metabolites, hormones, toxins, and nutrients.[1] In addition to the conventional T effector (Teff) and T regulatory (Treg) cells, T cells express many cytokines alone or in combination, such as $FOXP3^+$, $FOXP3^+IL\text{-}17^+$, $FOXP3^+IFNg^+$, and $FOXP3^+IL\text{-}17^+IFNg^+$, are encountered at the site of inflammation.[2] It is a fine balance of proinflammatory and anti-inflammatory cells, which, under autoimmune conditions, create a cytokine milieu promoting the conversion of Tregs into intermediate subsets (pro-inflammatory type). Tregs exhibit abnormalities in number, function, and expression profile in autoimmune conditions and transdifferentiate into a proinflammatory phenotype.[2] In type 1 diabetes (T1D), Tregs undergo increased apoptosis, exhibit unstable FOXP3 expression, and increase the frequency of intermediate Tregs that produce proinflammatory cytokines such as IFNg and IL-17.[3] Pathological conversion of Tregs that secrete IFNg, or T helper (Th)17 (intermediate state) establishes the importance of intermediate Treg cell types and plastic fate of Tregs in autoimmune diabetes, experimental autoimmune encephalitis (EAE), and autoimmune arthritis.[2,4,5] We aimed to exploit this flexible behavior exhibited by Tregs in autoimmune conditions and revert it to a nonpathogenic stable Treg state using immunomodulators, N1-guanyl-1,7-diaminoheptane (GC7) and anti-Delta-Like Ligand 4 (DLL4).

GC7 is the most potent inhibitor of deoxyhypusine synthase (DHS), an enzyme responsible for hypusination (post-translational addition of amino acid hypusine) and the functional activation of eukaryotic initiation factor 5a (eIF5a). eIF5a is a 17kDa conserved protein that was initially identified as a translational factor. Its function is context-dependent and is responsible for the nucleocytoplasmic shuttling of specific proteins and mRNAs primarily associated with proinflammatory markers such as iNOS, IFNg, dendritic cell maturation marker CD83, and M1 macrophage hallmarks.[6] Interestingly, the gene encoding eIF5a is found at diabetes-susceptibility loci in both mice and humans.[7] Hypusinated eIF5a (hyp-eIF5a) is overexpressed in T1D, contributing to the proinflammatory cytokine milieu and exacerbating endoplasmic reticulum (ER) stress.[8] Reports of hyp-eIF5a inhibition using GC7 have confirmed the impairment of proinflammatory polarization of Th1 immune cells and cytokine-mediated dysfunction in NOD mice,[9] a spontaneous humanized mouse model of T1D,[10–12] and human islets in vitro.[13]

Notch is a conserved cell-to-cell signaling network that plays a prominent role in T cells' maturation, activation, and differentiation.[14,15] The Notch ligand DLL4 inhibits the JAK3/STAT5 activation pathway that is necessary for FOXP3 expression and maintenance.[16] Inhibition of Notch signaling with anti-DLL4 results in the alternative differentiation and expansion of Tregs in NOD, humanized T1D mice,[12,17] and EAE.[16] Furthermore, Notch signaling plays a critical role in Treg differentiation independent of the thymus.[18] It has emerged as an essential regulator of RORγt and IL-23r genes, leading to the differentiation and activation of Th17 cells.[19] Thus, the data strongly indicate that Notch and eIF5a support a proinflammatory phenotype, and therapeutic interventions to inhibit this cascade could reset the immune imbalance in T1D/LADA and other autoimmune diseases.

In this manuscript, we, for the first time report the significant presence of the $CD4^+CD25^-IFNg^+IL17^+FOXP3^+$ intermediate Treg subset in patients with recent-onset T1D/LADA, which plasticized into conventional Tregs by GAD65 +GC7+anti-DLL4 treatment. Newly plasticized Tregs showed stable $CD25^+FOXP3^+$ expression and suppressed autologous T effector/Tresp cells. Moreover, GC7+anti-DLL4 treatment had no adverse effects on immune cells, encouraging further exploration of the simultaneous inhibition of Notch and eIF5a to restore immune imbalance in T1D/LADA and other autoimmune disorders.

Methods

Patient Recruitment

Healthy adults (n=7) and patients with T1D/LADA (n=7) signed informed consent forms and were enrolled in this study, which was approved by the Institutional Review Board of the University of Toledo. Specifically, T1D/LADA patients with positive titers of GAD65 autoantibodies were enrolled in this study. Minors (<18 years) and patients with a history of T1D/LADA (> 5 years) were excluded from the study. The study procedures included recording the

disease history, onset time, baseline HbA1c measurement, serum titers of GAD65 autoantibodies upon diagnosis, and mean daily insulin dosing requirements. The body mass index (BMI) was calculated using the ADA BMI calculator.

Characterization of Intermediate Tregs from Patients with T1D/LADA and Healthy Adults

Peripheral blood (10–20 mL) was collected in heparinized tubes, and mononuclear cells (PBMCs) were isolated using the Ficoll density gradient method. $CD4^+$ T cells were isolated from PBMCs using a $CD4^+$ T-cell isolation kit (Miltenyi Biotech), according to the manufacturer's protocol (Supplementary material S1 and Figure 1). Furthermore, $CD4^+CD25^+$ T cells and $CD4^+CD25^-$ T cells were column purified using a Treg isolation kit (Miltenyi Biotech) and analyzed by flow cytometry to quantify proinflammatory cytokines ($IFNg^+IL17^+FOXP3^+$) expressing intermediate Tregs (Figure 1).

Plasticization of Treg Deficient $CD4^+$ ($CD4^+CD25^-$) T Cells and CD4 Deficient PBMCs

The isolated $CD4^+CD25^-$ T cells were separated into batches of GAD65+GC7+anti-DLL4, anti-CD3/28/137 stimulation, and RPMI+20% FCS (control) groups for each treatment, maintained at 37°C and 5% CO_2 for seven days, and investigated for T-cell plasticity (Figure 2A and Supplementary material S2). For time-course analysis, at 96 h, a batch of cells from each treatment group was processed for flow cytometry to identify the different cell subsets. After 7 days, cells in each group were quantified by flow cytometry for the presence of plasticized $CD4^+CD25^+$ T cells, $CD4^+CD25^-$ T cells, and their respective proliferation (Figure 2 and Supplementary material S2).

Similarly, CD4-deficient PBMCs were divided into three groups and cultured under the indicated treatment conditions described above (Figure 3 and Supplementary material S2).

Suppression Assay of Plasticized Tregs and Autologous Naïve T Responsive Cells

Plasticized $CD4^+CD25^+$ Tregs were isolated using a Treg isolation kit from the cells cultured for 7 days under indicated treatment conditions (Supplementary material S3). Simultaneously, $CD4^+CD25^-$ T cells (Tresp cells) were isolated from freshly withdrawn peripheral blood of autologous patients, as described earlier. A suppression assay (n=4, repeated three times in triplicate) was performed using 1:0, 1:1, 1:2, and 0:1 ratios of plasticized $CD4^+CD25^+$ T cells from all three treatment groups: naïve/fresh $CD4^+CD25^-$ T cells (Tresp), as per the suppression assay protocol[20] (Figure 4 and Supplementary material S3). After 5 days, the cells were stained with CD4 and CD25 antibodies, and the proliferation of Tregs and Tresp was assessed according to the manufacturer's protocol[20] (Supplementary materials S3 and S4).

Similarly, an in vitro suppression assay (n=4, in triplicate repeated three times) was performed with $CD4^+CD25^+$ T cells plasticized from CD4 T cell-deficient PBMCs cultured under the indicated treatment conditions, against freshly isolated Tresp cells from autologous patients at different Treg: Tresp ratios (Figure 5). After 5 days of co-culture, cell proliferation was traced using the CFSE dye (Supplementary material S4), and the Treg phenotype was confirmed by flow cytometry, as previously described.

Assessment of Live, Dead, and Apoptotic Cell Populations After Immunomodulatory Treatment

Treg-deficient $CD4^+$ ($CD4^+CD25^-$) T cells and CD4-deficient PBMCs (n=6-8 in triplicate, repeated twice) were assessed for live, dead, and apoptotic cells following immunomodulatory treatment. One batch of cells was treated with GAD65 +GC7+anti-DLL4, whereas the other batch was suspended in RPMI+20% FCS (control) (Figures 6 and 7). Cells were cultured for seven days, and live, dead, and apoptotic cells were quantified using PO-PRO-1 and 7 amino actinomycin D, as per protocol (Figure 6, 7 and Supplementary material S5).

Quantification of TGF Beta (TGF-β) Concentration in the Cell Culture Supernatant

Human TGF beta1 ELISA Kit (Invitrogen cat# BMS249-4) was used to quantify TGF-β concentration in the cell culture supernatant after seven days of treatment with GAD65+GC7+anti-DLL4, according to the manufacturer's instructions.

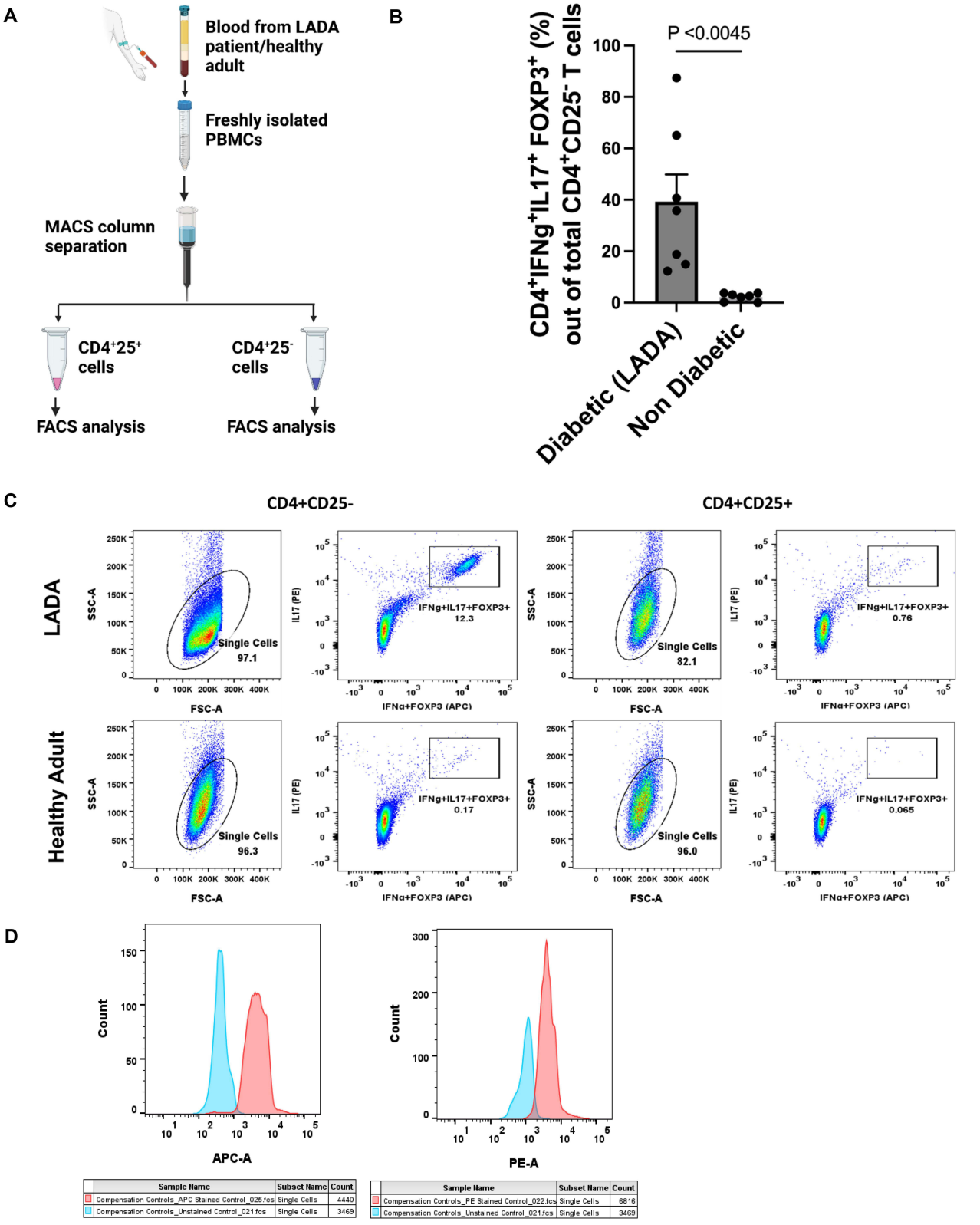

Figure 1 Characterization of Intermediate Tregs from patients with T1D/LADA and healthy adult donors (**A**) Isolation of peripheral blood mononuclear cells (PBMCs) from peripheral blood of patients with T1D/LADA and adult healthy controls (n=7 each) and column separation of $CD4^+CD25^-$ and $CD4^+CD25^+$ T cells to quantify $CD4^+IFNg^+IL17^+FOXP3^+$ intermediate Treg cell population (Created with BioRender.com) (**B**) Significantly elevated $CD4^+IFNg^+IL17^+FOXP3^+$ intermediate Treg population in T1D/LADA patients. (**C**) Dot plots of $CD4^+IFNg^+IL17^+FOXP3^+$ intermediate Tregs in $CD4^+CD25^-$ and $CD4^+CD25^+$ T cell subsets representative of significantly increased intermediate $CD4^+CD25^-IFNg^+IL17^+FOXP3^+$ Tregs in T1D/LADA patients. (**D**) Unstained and single-stained controls for APC and PE. The statistical significance threshold was set at $P \leq 0.05$. Data are presented as the means ± standard error of means (SEM).

Flow Cytometry

All flow cytometry analyses were performed using at least 25000 live cells. Our established immunofluorescence staining protocol was executed for flow cytometry experiments involving cell surface and intracellular staining[10–12,21–23] (Supplementary Material S6, and compensation controls in Supplementary Material S7). The data were analyzed using the FlowJo software.

Statistical Analysis

Statistical analyses were performed using the GraphPad Prism 10.2. Student's *T*-test was used to establish the statistical significance for the proportion of intermediate Tregs in T1D/LADA patients and healthy controls. One-way ANOVA was

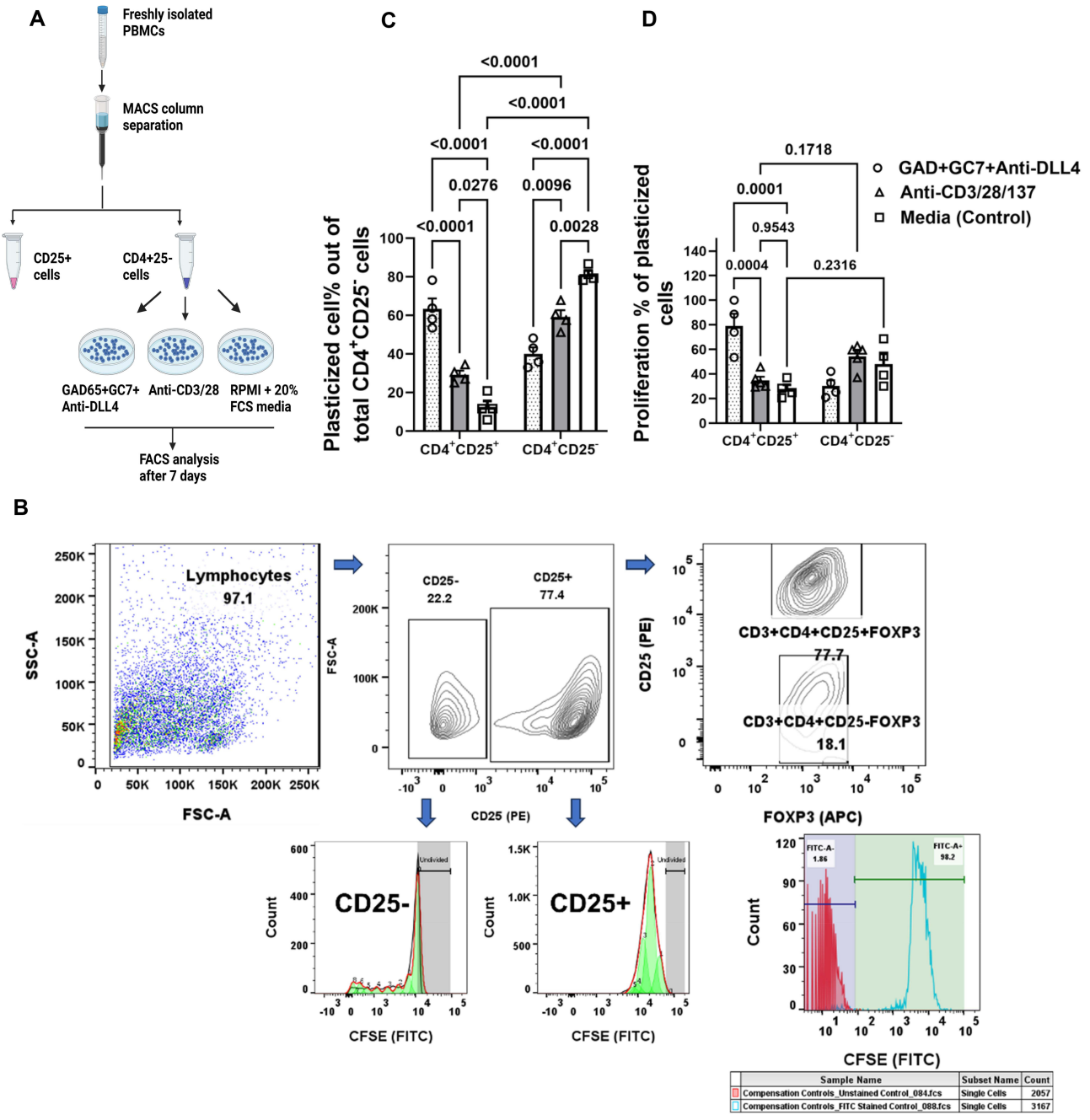

Figure 2 Continued.

https://doi.org/10.2147/ITT.S504555

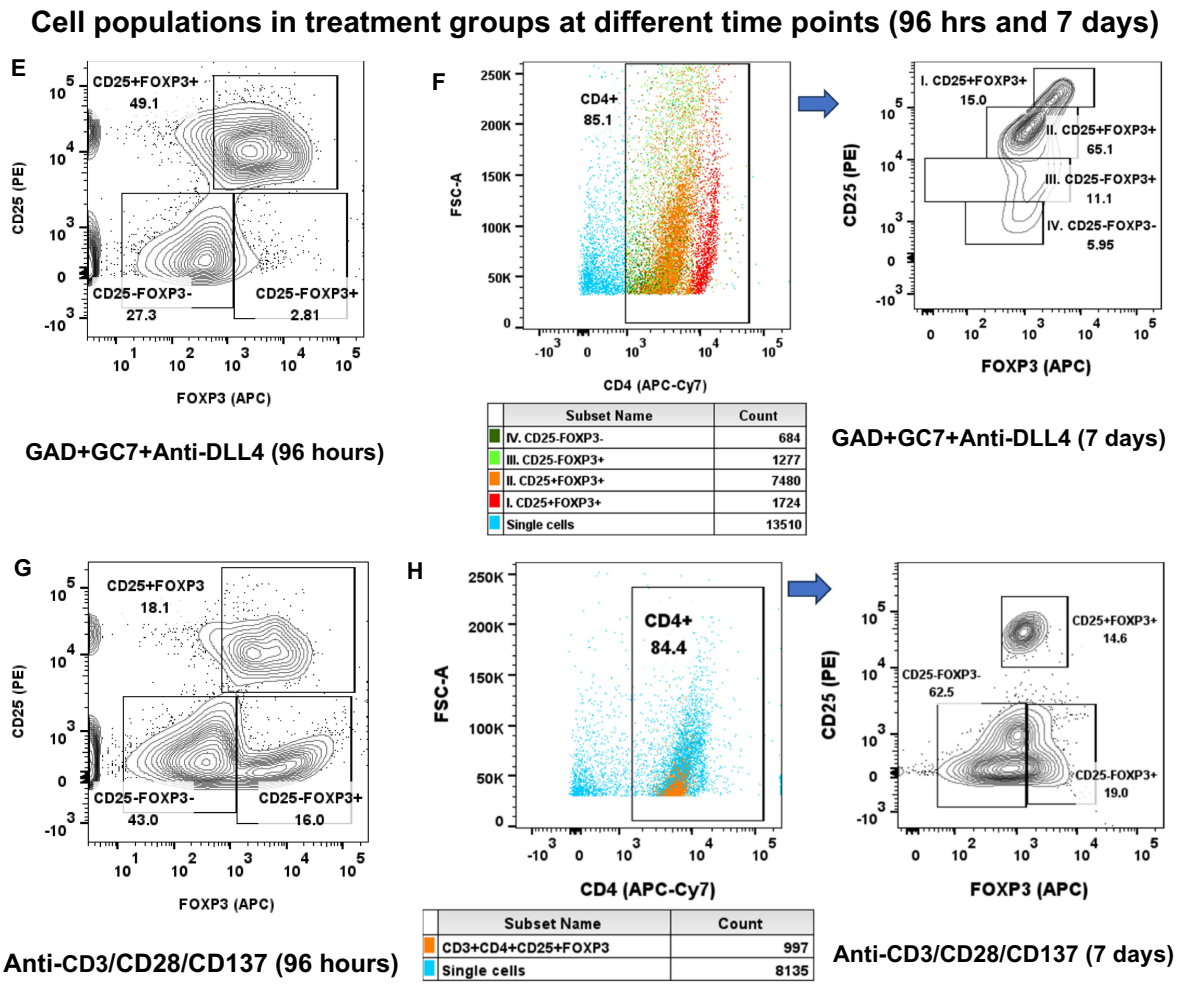

Figure 2 Continued.

used to analyze the effect of different treatments on cell plasticity and proliferation, followed by multiple comparisons using Tukey's multiple comparison test. The threshold for statistical significance was set at $P \leq 0.05$. Data are presented as the mean ± standard error of the mean (SEM).

Results

$CD4^+CD25^-IFNg^+IL17^+FOXP3^+$ Tregs are Significantly Increased in Recent-Onset T1D/LADA Patients

The baseline characteristics of patients with recent-onset T1D/LADA (n=7) and healthy controls (n=7) are presented in Table 1. Age and BMI did not differ significantly (*t*-test, P value >0.50 for both comparisons). The phenotypic immune cell profiling of $CD4^+CD25^+$ and $CD4^+CD25^-$ T-cell subsets revealed significantly increased numbers of $CD4^+$ T cells expressing $IFNg^+IL17^+FOXP3^+$ (39.29±10.6%) in the Treg-deficient ($CD4^+CD25^-$) T-cell pool of patients with T1D/LADA. In contrast, 2.23±0.6% were present in healthy controls (Figure 1A–D and Supplementary material S8).[24] This finding is instrumental since in healthy human adults, the percentage of $CD4^+$ T cells expressing FOXP3 in peripheral blood is about 8.6±1.7%, of which 3.2±1.1% express IL-17.[25] These $CD4^+CD25^-IFNg^+IL17^+FOXP3^+$ cells can be deemed as transient Tregs (intermediate differentiation subset of unfit Tregs that have acquired T effector (Teffs) phenotype and/or are not terminally differentiated)[26,27] or Teffs expressing FOXP3, since human Teffs transiently express intermediate levels of FOXP3.[28] Based on our previous studies, we envisioned the plasticization of intermediate

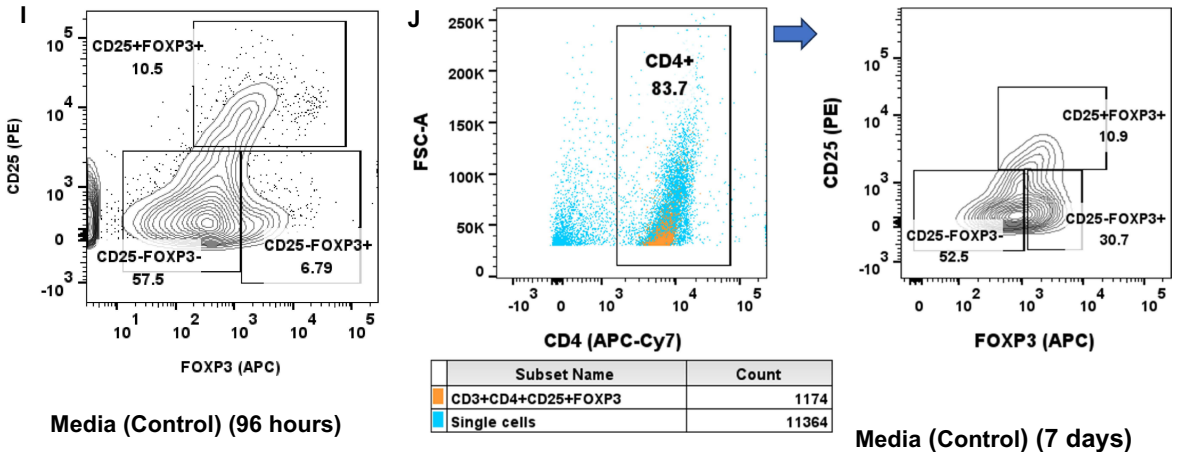

Figure 2 GAD65+GC7+anti-DLL4 treatment plasticizes $CD4^+CD25^-$ T cells into $CD4^+CD25^+$ T cells (**A**) Workflow diagram of isolation of $CD4^+CD25^-$ T cells from PBMCs and culture with GAD65+GC7+anti-DLL4, anti-CD3/28/137 stimulation and media (RPMI+20%FCS) to investigate the conversion of $CD4^+CD25^-$ T cells into $CD4^+CD25^+$ T cells and their proliferation index (Created with BioRender.com). (**B**) Representative contour diagram and histogram of 3 independent experiments (n=4, in triplicate) of $CD25^+$ and $CD25^-$ T cells sorted from $CD4^+$ T cells and their proliferation assessed by CFSE (FITC) dye after 7 days of GAD65+GC7+anti-DLL4 treatment. The sorted $CD4^+$ cells (leftmost quadrant) were gated based on CD25 positivity (at the center). Further, these $CD4^+$ cells were also gated for $CD25^+$ (PE) and $FOXP3^+$ (APC) expression simultaneously to confirm that almost all plasticized $CD25^+$ cells (77.4%) are $FOXP3^+$ (rightmost top quadrant). Unstimulated CFSE (FITC) control is also given. (**C**) Percentage of $CD4^+CD25^-$ T cells plasticizing into $CD4^+CD25^+$ T cells under GAD65+GC7+anti-DLL4, anti-CD3/28/137 stimulation, and culture media condition (**D**) Proliferation percentage of $CD4^+CD25^+$ T cells and $CD4^+CD25^-$ T cells in different treatment groups. $CD4^+CD25^+$ T cells that were plasticized under antigen-specific GAD65+GC7+anti-DLL4 treatment had better proliferation capacity. (**E**) Contour plot of $CD4^+CD25^-$ T cells undergoing plasticity at 96 hrs after GAD65+GC7+anti-DLL4 treatment. (**F**) Dot plot of $CD4^+CD25^-$ T cells at different stages of plasticization, transitioning into $CD4^+CD25^+$ $FOXP3^+$ Tregs cells after seven days of treatment. Four types of $CD4^+$ T cell populations are visible in the GAD65+GC7+anti-DLL4 group viz. $CD25^-FOXP3^-$ (IV), $CD25^-FOXP3^+$(III), $CD25^+FOXP3^+$ (II) and $CD25^{+high}FOXP3^{+high}$ (**I**). $CD25^-FOXP3^-$ (IV. green) and $CD25^-FOXP3^+$ T cells (III. light green) transitioning into $CD25^+FOXP3^+$ (II. Orange color) and $CD25^{+high}FOXP3^{+high}$ T cells (I. red color). The $CD25^{+high}FOXP3^{+high}$ (I. red color) is an entirely distinct population, showing high expression of CD25 and FOXP3, that has transdifferentiated from the intermediate Tregs ($CD4^+CD25^-IFNg^+IL17^+FOXP3^+$). (**G**) Contour plot of $CD4^+CD25^-$ T cells at 96 hrs after anti-CD3/28/137 stimulation. (**H**) Dot plot of $CD4^+CD25^-$ T cells at 7 days after anti-CD3/28/137 stimulation. (**I**) Contour plot of $CD4^+CD25^-$ T cells at 96 hrs in culture media. (**J**) Dot plot of $CD4^+CD25^-$ T cells culture media after 7 days.

Notes: In the anti-CD3/28/137 stimulation and media group (**H** and **J**), only three cell populations are noticeable viz. $CD25^+FOXP3^+$, $CD25^-FOXP3^+$ and $CD25^-FOXP3^-$. The statistical significance threshold was set at $P \leq 0.05$. Data are presented as the means ± standard error of means (SEM).

$CD4^+CD25^-IFNg^+IL17^+FOXP3^+$ Tregs into stable Tregs by inhibition of eIF5a and Notch pathways based on our previous studies.[10–12]

GAD65+GC7+anti-DLL4 Treatment Plasticizes $CD4^+CD25^-$ T Cells Into $CD4^+CD25^+$ T Cells

To further ascertain the origin of $CD4^+CD25^-IFNg^+IL17^+FOXP3^+$ T cells and to induce plasticity in these intermediate Tregs, we isolated PBMCs from patients with recent-onset T1D/LADA. We sorted the pure population of $CD4^+CD25^-$ T cells, rendered the $CD4^+$ T cell pool completely devoid of $CD25^+$ T cells, and subjected the cells to simultaneous immunomodulatory treatment with GAD65+GC7+anti-DLL4 (Figure 2A). Any $CD4^+CD25^+$ T cells in this cell pool must have a $CD4^+CD25^-$ origin and immunomodulatory treatment rewires $CD4^+CD25^-IFNg^+IL17^+FOXP3^+$ T cells into $CD4^+CD25^+FOXP3^+$ Tregs. After seven days of immunomodulatory treatment, we identified a significant increase in the number of $CD4^+CD25^+$ T cells in the GAD65+GC7+anti-DLL4 treated group, indicating that $CD4^+CD25^-$ T cells undergo plasticity changes and are in the process of expressing the Treg phenotype ($CD4^+CD25^+FOXP3^+$) (Figure 2B and C). Figure 2E–J is a time course analysis (96 hours and 7 days) of the cultured cells under different treatment groups and shows the transition of cells from $CD4^+CD25^-$ T cells to $CD4^+25^+FOXP3^+$ T cells with different intermediate populations developing at different time points. As is evident on 7th day post-treatment in a representative Figure 2F, four types of cell populations are present in the GAD65+GC7+anti-DLL4 treated group viz. $CD25^-FOXP3^-$ (IV), $CD25^-FOXP3^+$(III), $CD25^+FOXP3^+$ (II), and $CD25^{+high}FOXP3^{+high}$ (I), wherein $CD25^-$ T cells (III, IV. green) transitioned into $CD25^+FOXP3^+$ cells (II. orange), and $CD25^{+high}FOXP3^{+high}$ (I. red). Therefore, in the antigen-specific GAD65+GC7+anti-DLL4 treated group, a significant number of $CD4^+CD25^-$ T cells (63.4± 5.4%) plasticized into $CD4^+CD25^+$ T cells (Figure 2C) and had significantly higher proliferative capacity (Figure 2D). In contrast, in the

https://doi.org/10.2147/ITT.S504555

conventional anti-CD3/28/137 stimulation group, 29.3±2.0% of $CD4^+CD25^-$ T cells plasticized into $CD4^+CD25^+$ T cells (Figure 2C); however, the proliferative capacity of $CD4^+CD25^+$ T cells was significantly lower ($P<0.0004$) than that of the GAD65+GC7+anti-DLL4 treated group (Figure 2D). Moreover, approximately 12.5±3.1% of $CD4^+CD25^-$ T cells in the culture media (RPMI+20% FCS) group plasticized into $CD4^+CD25^+$ T cells (Figure 2C). Since Tregs constitute only a small fraction of T cells in human peripheral blood (5%), in the culture media (control group) where cells were cultured in a neutral environment (RPMI+20%FCS), these "intermediate" cells were able to revert to their original Treg phenotype. This suggests that the differentiation from $CD4^+CD25^-$ T cells to $CD4^+CD25^+$ T cells is a phenomenon of cellular homeostasis, but in response to the proinflammatory milieu of T1D/LADA (Supplementary material S9A and B), these cells were unable to sustain the Treg phenotype. This is a widely observed event in T1D/LADA and other autoimmune diseases, in which Tregs exhibit unstable FOXP3 expression and pathological conversion of $FOXP3^+$ into $FOXP3^+IL17^+$ and $FOXP3^+IFNg^+$ T cells.[3,5,25]

We assessed the proliferation index of cells undergoing plasticity after 7-days of treatment (Figure 2D). The percentage proliferation of plasticized $CD4^+CD25^+$ T cells was significantly higher ($P=0.0004$) in the GAD65+GC7 +anti-DLL4 treatment group (79.0%) than that in the other groups (34.8% in anti-CD3/28/137 stimulation, 27.7% in media conditions, Figure 2D). Although there was a considerable proportion of plasticized $CD4^+CD25^+$ T cells in the anti-CD3/28/137 stimulation and culture media groups (Figure 2C), the plasticized ($CD4^+CD25^+$) T cells in these groups proliferated less, resulting in a higher proliferation index of $CD4^+CD25^-$ T cells (Figure 2D).

$CD4^+CD25^-IFNg^+IL17^+FOXP3^+$ T cells proliferated differentially and significantly under antigenic stimulation in the GAD65+GC7+anti-DLL4 treated group since the cells were activated in an antigen-specific manner[29] and underwent reprogramming towards the Treg phenotype (Figure 2E and F). In contrast, the blunt activation under anti-CD3/28/137 stimulation resulted in a generalized T-cell activation wherein intermediate cells expressed the $CD25^+$ phenotype after strong activation of $CD4^+$ T cells (ie, physiological feedback expression of $CD25^+$ receptor to inhibit over-activation of $CD4^+$ T cells),[30] as observable in Figure 2H and J wherein in the anti-CD3/28/137 stimulation and media group, only three cell populations are noticeable viz. $CD25^+FOXP3^+$, $CD25^-FOXP3^+$ and $CD25^-FOXP3^-$ T cells. Therefore, we can speculate that the evolution of $CD4^+CD25^+$ T cells in the GAD65+GC7+ anti-DLL4 treated group was different from that in the anti-CD3/28/137 stimulation and media groups, as is evident in the dot plot (Figure 2F), where four different populations of $CD4^+$ cells were visible {$CD25^-$ (IV, III. green) and transitioning to $CD25^+FOXP3^+$ (II. orange), and $CD25^{+high}FOXP3^{+high}$ (I. red)}. This reprogramming hypothesis was again validated in our study by plasticizing CD4 deficient PBMCs, where $CD8^+$ T cells first dedifferentiated and then re-differentiated into $CD4^+CD25^+FOXP3^+$ T cells, as explained in later sections.

GAD65+GC7+anti-DLL4 Treatment Plasticizes CD4 Deficient PBMCs into $CD4^+CD25^+FOXP3^+$ Tregs Withstanding Proinflammatory Milieu

We mimicked the human T1D/LADA proinflammatory microenvironment to investigate further whether combination treatment with GC7+anti-DLL4 could plasticize $CD8^+$ T cells from CD4 deficient PBMCs into Tregs, withstand proinflammatory conditions, and be capable of plasticizing cells independently of the cytokine milieu. We sorted $CD4^+$ T cells from the PBMCs of T1D/LADA patients and harvested CD4 T cell-deficient PBMCs (Figure 3A and B). This cell population consists of $CD8^+$ T cells and antigen-presenting cells (APCs), such as monocytes, neutrophils, dendritic cells, and natural killer (NK) cells, which are responsible for the activation of $CD8^+$ T cells into cytotoxic T lymphocytes (CTLs; $CD8^+$ T cells producing IFN-g), generating a proinflammatory cytokine milieu (Supplementary material S9B). CD4 deficient PBMCs were subjected to GAD65+GC7+anti-DLL4 treatment for seven days, wherein the GAD65 antigen was recognized and presented by APCs to GAD65 specific $CD8^+$ T cells and activated into CTLs (Teffs), as in the T1D/LADA condition. Seven days after GAD65+GC7+anti-DLL4 treatment, the phenotype of cells was analyzed by flow cytometry, which clearly revealed that 20.3±3.1% of $CD8^+$ T cells plasticized to $CD4^+$ T cells (Figure 3C and D). These plasticized $CD4^+$ T cells further underwent differentiation, and 45.6±8.8% of these $CD4^+$ T cells expressed the $CD25^+FOXP3^+$ phenotype (Figure 3C, E and G). As explained earlier, the possible mechanism is the dedifferentiation of $CD8^+$ T cells into double-negative/double-positive T cells, followed by redifferentiation into single-positive $CD4^+$ T cells expressing a regulatory phenotype ($CD25^+FOXP3^+$) (data not shown). Moreover, 9.0±1.0%

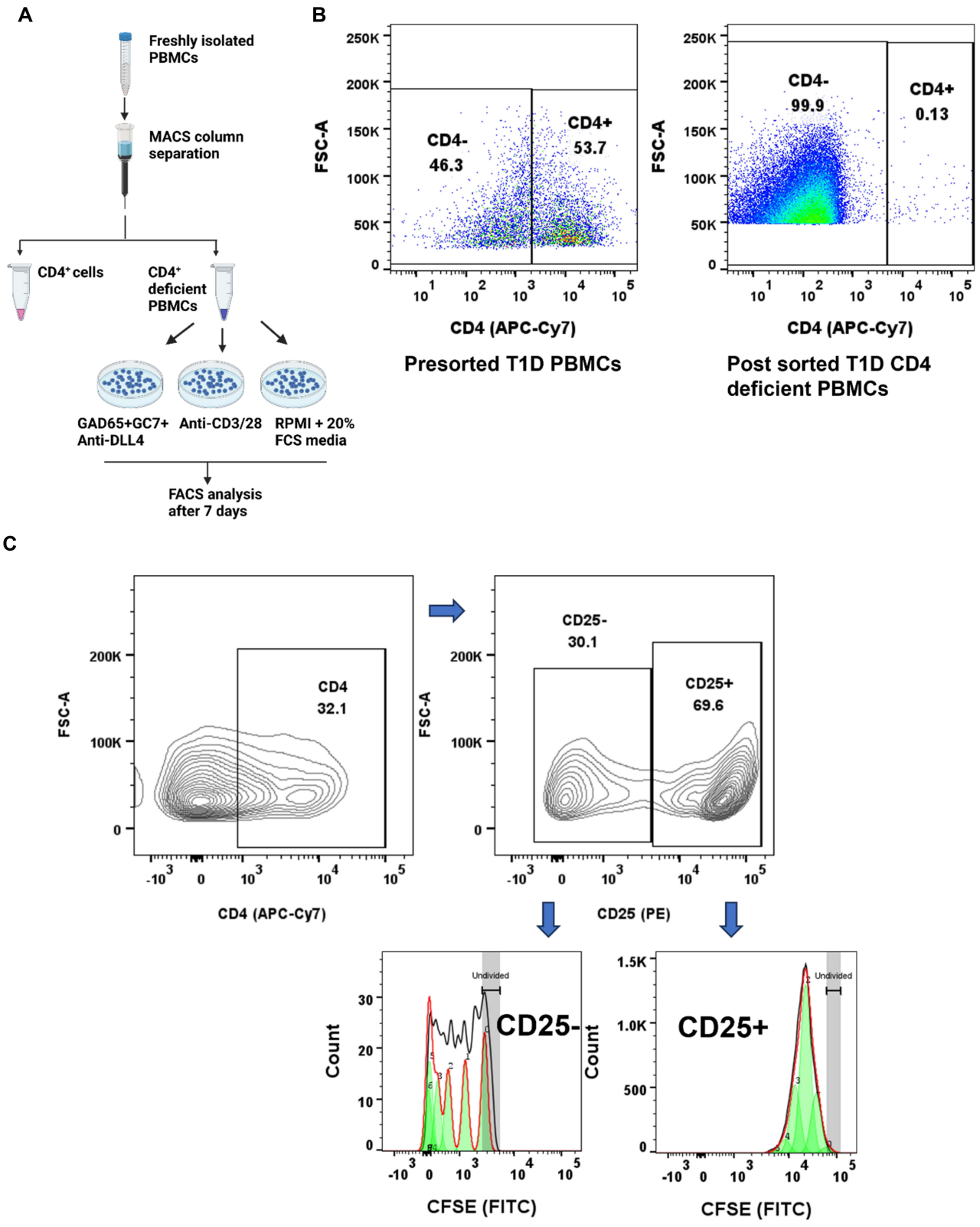

Figure 3 Continued.

https://doi.org/10.2147/ITT.S504555

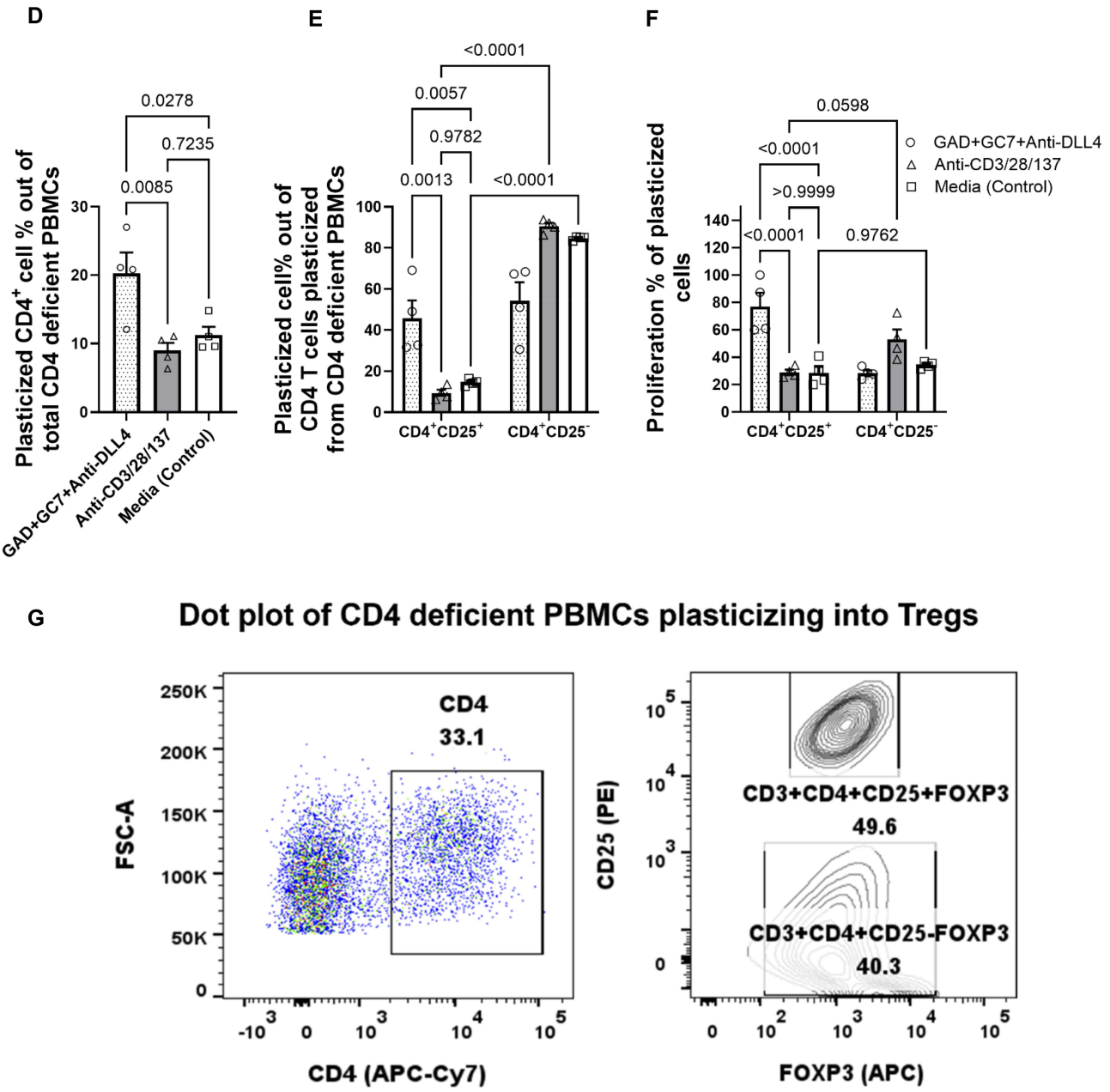

Figure 3 GAD65+GC7+anti-DLL4 treatment plasticizes CD4 deficient PBMCs into $CD4^+CD25^+FOXP3^+$ Tregs withstanding proinflammatory milieu mimicking T1D/LADA. (**A**) Workflow diagram of isolation of $CD4^+$ T cells from PBMCs and culture of CD4 deficient PBMCs with GAD65+GC7+anti-DLL4, anti-CD3/28/137 stimulation and culture media (RPMI+20%FCS) (Created with BioRender.com). (**B**) A representative image of gated $CD4^+$ and $CD4^-$ T cells in the PBMCs of T1D/LADA patients before (left quadrant) and after MACS column sorting (right quadrant). (**C**) A representative image of 3 independent experiments (n=4, in triplicate) showing Contour diagram of plasticized $CD4^+$ T cells from CD4 deficient PBMCs (left quadrant). $CD25^+$ and $CD25^-$ cells were gated from plasticized $CD4^+$ T cells (upper right quadrant), and their proliferation was assessed by CFSE (FITC) dye (histogram, lower right quadrant). (**D**) Percentage of $CD4^+$ T cells plasticized from CD4 deficient PBMCs cultured for 7 days under GAD65+GC7+anti-DLL4, anti-CD3/28/137 stimulation, and culture media conditions. (**E**) Percentage of $CD4^+CD25^-$ and $CD4^+CD25^+$ T cells derived from plasticized $CD4^+$ T cells with indicated treatments. (**F**) Proliferation percentage of $CD4^+CD25^-$ T and $CD4^+CD25^+$ T cells derived from different treatment conditions. (**G**) Representative Dot plots and contour diagram of 3 independent experiments of CD4 deficient PBMCs plasticizing first into $CD4^+$ T cells followed by further transdifferentiation into $CD4^+CD25^+FOXP3^+$ Tregs. The statistical significance threshold was set at $P \leq 0.05$. Data are presented as the means ± standard error of means (SEM).

and 11.2±1.2% of CD4 deficient PBMCs in anti-CD3/28/137 stimulation and media group, respectively, also plasticized into $CD4^+$ T cells (Figure 3D), which is an apparent phenomenon under physiological stimulations.[31] Furthermore, the newly plasticized $CD4^+CD25^+$ Tregs had a better proliferation potential than $CD4^+CD25^+$ Tregs plasticized from anti-CD3/28/137 stimulation ($P<0.0001$) and media groups ($P<0.0001$) (Figure 3F). The present data define the emergence of T-cell plasticity as an evolving paradigm shift in clinical immune cell biology.

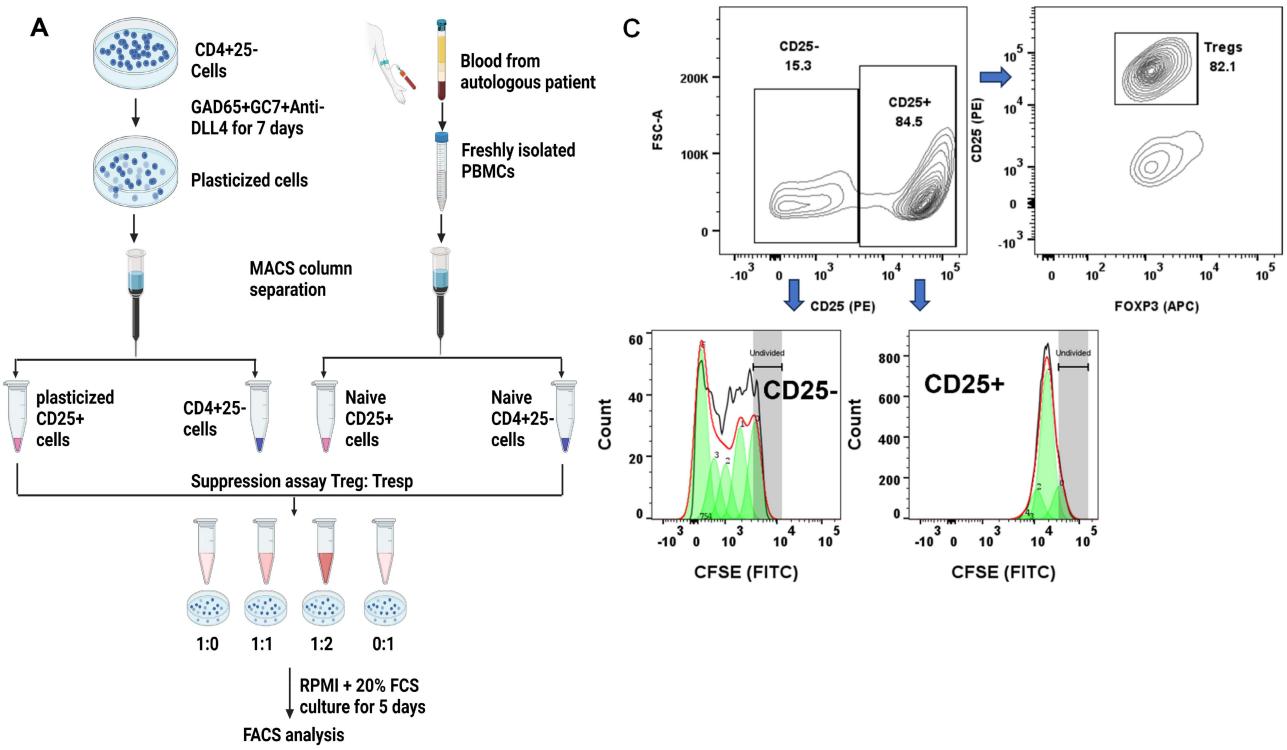

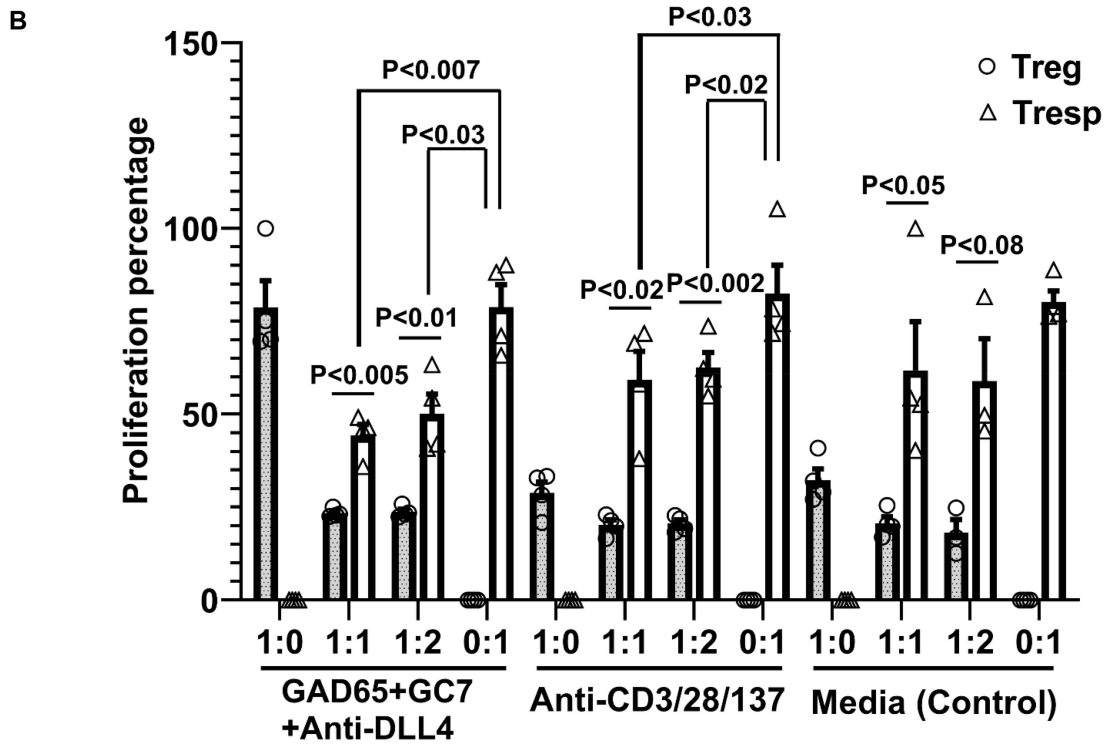

Figure 4 Plasticized $CD4^+CD25^+FOXP3^+$ Tregs cells exhibited a functional regulatory phenotype (**A**) Workflow diagram of isolation of plasticized $CD4^+CD25^+$ T cells derived from Treg deficient $CD4^+$ T cells cultured under GAD65+GC7+anti-DLL4, anti-CD3/28/137 stimulation, and media (RPMI+20%FCS) conditions followed by suppression assay against freshly isolated autologous Tresp ($CD4^+CD25^-$) cells in different ratios (Created with BioRender.com) (**B**) Proliferation percentage of plasticized Tregs and Tresp cells in different co-culture ratios in a suppression assay (n=4, in triplicate repeated 3 times). (**C**) Representative image of Contour diagram and histogram of sorted $CD25^+$ T cells and $CD25^-$ T cells cultured under GAD65+GC7+anti-DLL4 condition and their proliferation assessed by CFSE (FITC) dye post-5-day suppression assay. Notably, the Treg phenotype was maintained in the plasticized $CD4^+CD25^+$ T cells post-suppression assay. The statistical significance threshold was set at $P \leq 0.05$. Data are presented as the means ± standard error of means (SEM).

https://doi.org/10.2147/ITT.S504555

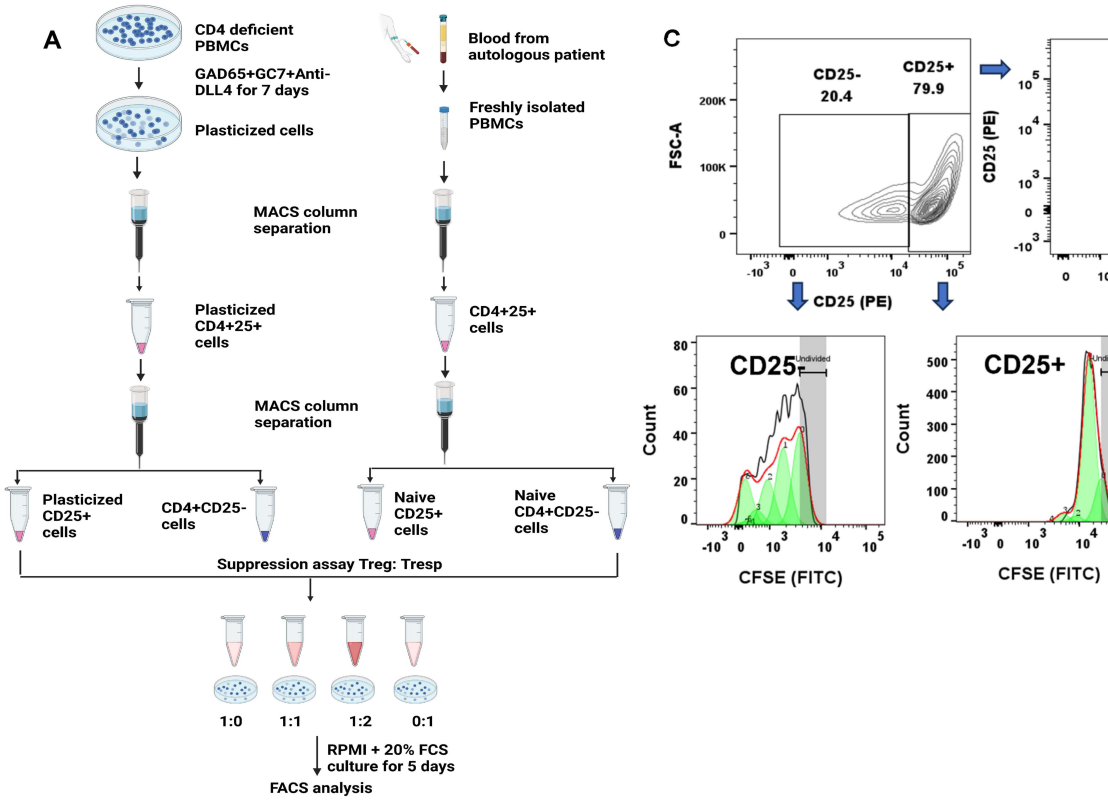

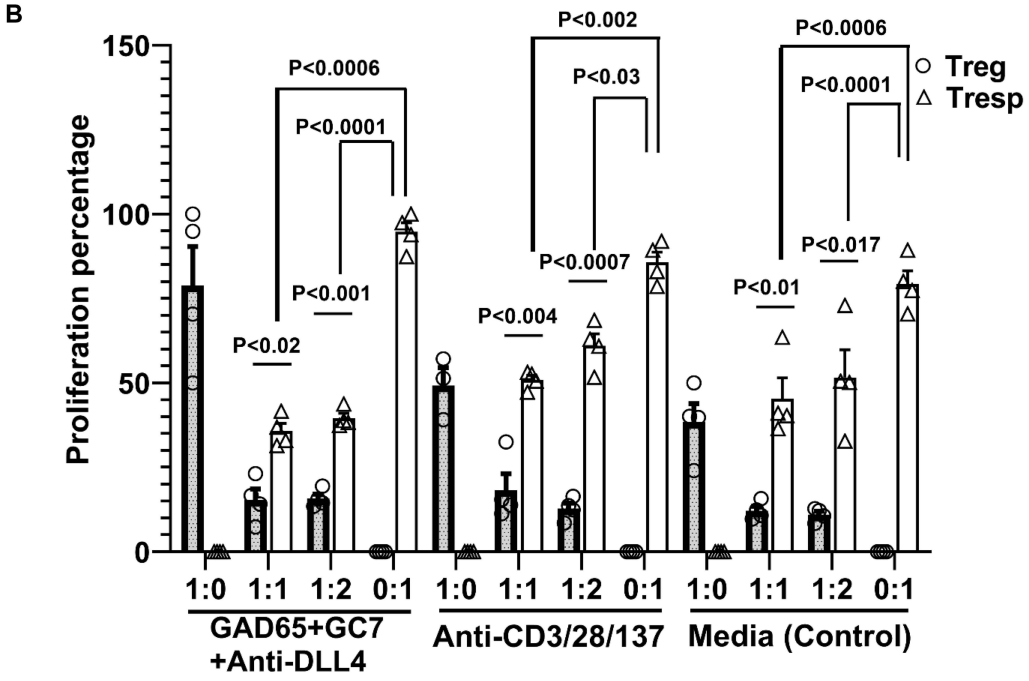

Figure 5 Plasticized $CD4^+CD25^+FOXP3^+$ Tregs cells from CD4 deficient PBMCs also exhibited a functional regulatory phenotype (**A**) Workflow diagram of isolation of plasticized $CD4^+CD25^+$ T cells from CD4 deficient PBMCs cells cultured under GAD+GC7+anti-DLL4, anti-CD3/28/137 stimulation, culture media (RPMI+20%FCS) conditions followed by suppression assay against freshly isolated autologous Tresp ($CD4^+CD25^-$ (T) cells in different co-culture ratios (Created with BioRender.com) (**B**) Proliferation percentage of Tregs (derived from GAD65+GC7+anti-DLL4, anti-CD3/28/137 stimulation, culture media group) and autologous Tresp cells in different ratios in a suppression assay (n=4, in triplicate repeated 3 times). (**C**) Representative contour diagram and histogram of sorted $CD25^+$ T cells and $CD25^-$ T cells and their proliferation assessed by CFSE (FITC) dye post-5-day suppression assay. Notably, the Treg phenotype was maintained in the plasticized CD4+CD25+ T cells post-suppression assay. The statistical significance threshold was set at $P \leq 0.05$. Data are presented as the means ± standard error of means (SEM).

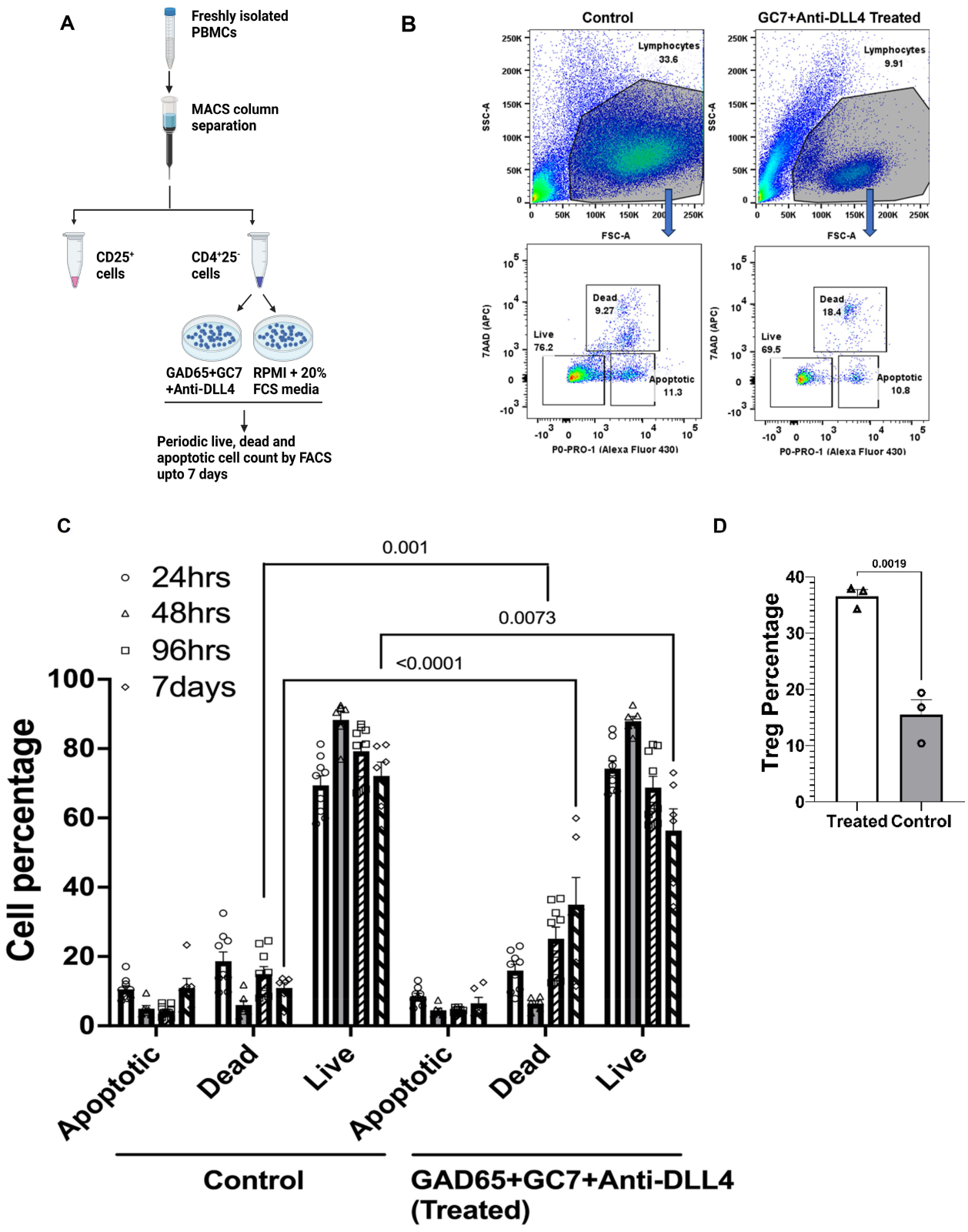

Figure 6 Continued.

https://doi.org/10.2147/ITT.S504555

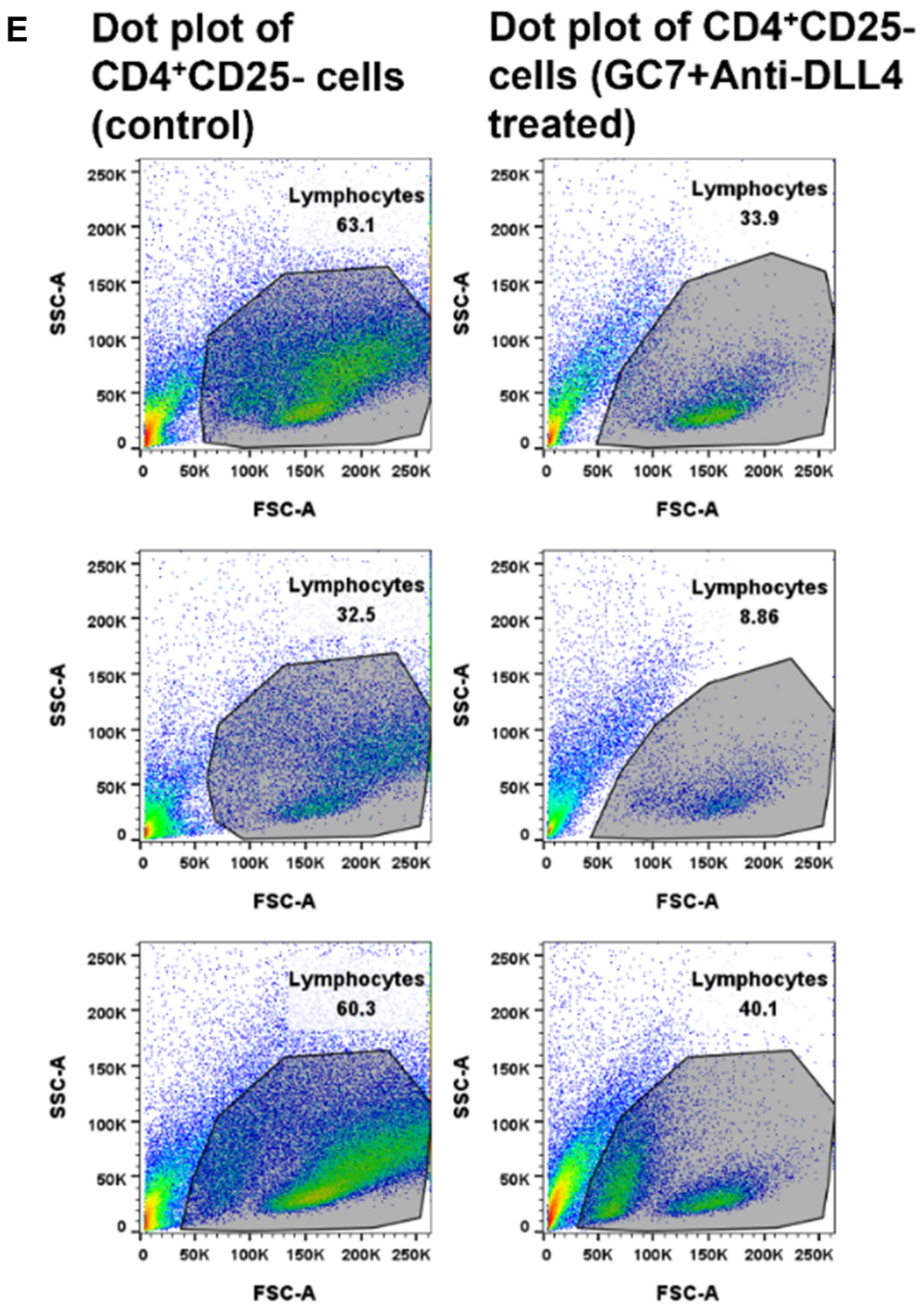

Figure 6 No adverse effects of immunomodulatory GAD65+GC7+anti-DLL4 treatment on $CD4^+$ T cells (**A**) Workflow diagram of isolation of $CD4^+CD25^-$ T cells from PBMCs and culture with GAD65+GC7+anti-DLL4 and culture media (control) (Created with BioRender.com) (**B**) Sorting strategies of lymphocytes in control and treated group followed by gating strategy of live, dead and apoptotic cells. (**C**) Percentage of live, dead, and apoptotic cells in control and GAD65+GC7+anti DLL4 treatment group at 24, 48, 96 hours, and 7 days (n=6-8 in triplicate, repeated twice) (**D**) Treg cell percentage on 7^{th} day to determine the phenotype of live cells in treated and control group. (**E**) Representative dot plot of autologous $CD4^+CD25^-$ T cells cultured with GAD65+GC7+anti-DLL4 and control showing significant ($P<0.007$) live lymphocyte percentage in the control group Vs treated group. The statistical significance threshold was set at $P \leq 0.05$. Data are presented as the means ± standard error of means (SEM).

Plasticized Tregs ($CD4^+CD25^+FOXP3^+$) Cells Exhibited a Functional Regulatory Phenotype

Transforming growth factor β (TGF-β)-induced Tregs are unstable in sustaining in vivo suppression of Teffs, which limits their therapeutic application.[32–34] Moreover, in humans, activated T cells transiently upregulate $FOXP3^+$ without acquiring Treg phenotype and function.[35–38] Therefore, we investigated the functional regulatory phenotype of newly plasticized

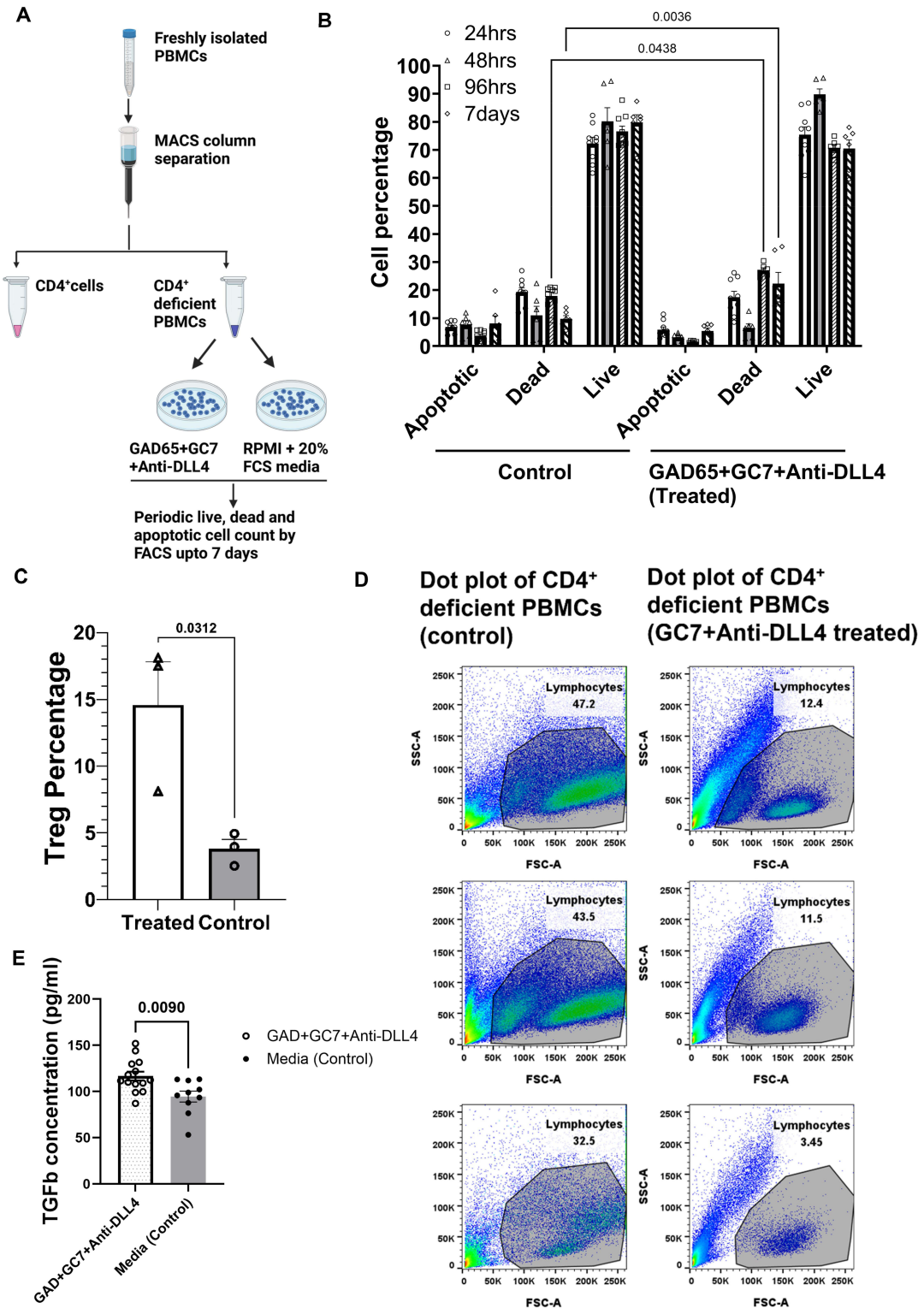

Figure 7 No adverse effects on cell viability of $CD8^+$ and other accessory cells in CD4 deficient PBMCs with immunomodulatory GAD65+GC7+anti-DLL4 treatment (**A**) Workflow diagram on the isolation of CD4 deficient PBMCs and culture with GAD65+GC7+anti-DLL4 and culture media (control) (Created with BioRender.com) (**B**) Percentage of live, dead and apoptotic cells in control and GAD65+GC7+anti-DLL4 treatment group at 24, 48, 96 hours and 7 days (n=6-8 in triplicate, repeated twice) (**C**) Treg cell percentage on 7^{th} day in GAD65+GC7+anti-DLL4 and control group. Significant enrichment of Tregs (P<0.03) in GAD65+GC7+anti-DLL4 treated group. (**D**) Dot plot of autologous CD4 deficient PBMCs cultured with GAD65+GC7+anti-DLL4 and control showing significant live lymphocyte percentage in control Vs treated group. (**E**) Increased TGF-β concentration in the cell culture supernatant in the GAD65+GC7+anti-DLL4 treatment group after 7 days. The statistical significance threshold was set at $P \leq 0.05$. Data are presented as the means ± standard error of means (SEM).

https://doi.org/10.2147/ITT.S504555

Table 1 T1D/LADA Patients/Controls List

Study ID	Age (years)	Gender	BMI (lb/in^2)	HbA_{1C} % (mmol/mol) at diagnosis	Anti- GAD65 Titer (IU/mL)	Insulin Dependency	Time from Diagnosis to Blood Collection	Diagnosis
1	45	F	17.75	12.1 (109)	>250	20 units	6 Months	T1D/LADA
2	39	M	21.44	9.4 (79)	98.0	40 units	2 Months	T1D/LADA
3	61	F	23.6	11.6 (103)	>250	40 units	4 Years	T1D/LADA
4	37	M	22.6	11.6 (103)	>250	60 units	3 Years	T1D/LADA
5	52	M	31.9	12.1 (109)	132.5	50 units	4 Months	T1D/LADA
6	38	M	24.89	14.1 (131)	>250	40 units	8 Months	T1D/LADA
7	22	M	17.28	14.8 (138)	>250	15 units	1 year	T1D/LADA
Mean±SE	**42±4.7**		**22.77±1.9**	**12.24±0.7**		**37.8±5.9**	**16.57±6.8 Months**	
8	22	M	26.5	<5.4	<5.0	N	N/A	Healthy control
9	36	F	21.2	<5.4	<5.0	N	N/A	Healthy control
10	36	M	25.2	<5.4	<5.0	N	N/A	Healthy control
11	45	M	22.9	<5.4	<5.0	N	N/A	Healthy control
12	37	F	27.9	<5.4	<5.0	N	N/A	Healthy control
13	62	M	27.3	<5.4	<5.0	N	N/A	Healthy control
14	43	M	28.1	<5.4	<5.0	N	N/A	Healthy control
Mean±SE	**40.14±4.6**		**24.68±0.7**					

$CD4^+CD25^+FOXP3^+$ cells from different treatment wells and evaluated their suppressive capacity against freshly isolated autologous naïve $CD4^+CD25^-$ Teffs (Figure 4A and B). Flow cytometry analysis of the cells after the suppression assay confirmed the Treg phenotype and significant suppression of Teffs (Figure 4B and C). The newly plasticized Tregs from GAD65+GC7+anti-DLL4 treatment demonstrated stable $CD25^+FOXP3^+$ expression after co-culture (Figure 4C, right quarter) and superior functional suppressive capacity against autologous Teffs (Figure 4B). Indeed, antigen-specific Tregs have superior suppression potential than polyclonal or blunt-activated Tregs.[29] It is noteworthy that the suppression assay was performed under culture conditions devoid of any IL-2 after thoroughly washing the cells with RPMI (three times). Therefore, the proliferation of $CD25^+$ T cells occurs in response to endogenous IL-2 secreted by $CD4^+CD25^-$ T cells, and the subsequent suppression of Teffs simulates the in vivo immune regulatory response.[39] These findings prove that newly plasticized Tregs have a stable $CD25^+FOXP3^+$ phenotype and a functional suppressive capacity.

Similarly, the newly plasticized Tregs from CD4 deficient PBMCs ($CD8^+$ T cells and APCs) were column purified, confirmed for the Treg phenotype ($CD4^+CD25^+FOXP3^+$), and co-cultured with freshly isolated autologous Teffs (Tresp, $CD4^+CD25^-$) at different ratios of Treg/Tresp 1:0, 1:1, 1:2, and 0:1, respectively (Figure 5A). Tregs plasticized from the GAD65+GC7+anti-DLL4 group significantly suppressed Teffs (Figure 5B and C). Notably, the Tregs that were plasticized from the conventional anti-CD3/28/137 stimulation group and the culture media (control) group also exhibited significant suppression, which is the physiological role of Tregs. However, in pathological conditions (such as T1D/LADA), there is a derangement of Treg: Tresp ratios; therefore, Tregs cannot effectively suppress Teffs. As the

ratio of Tresp: Tregs was the same in all three groups, the Tregs plasticized from the anti-CD3/28/137 and media groups also exhibited significant suppression of Tresps (Figure 5B).

Immunomodulatory GC7+anti-DLL4 Treatment Did Not Have Any Adverse Effects on the Immune Cells

In vivo studies on T1D[11,12] and NOD mice[17] did not reveal any significant adverse effects of GC7 or anti-DLL4. However, to validate the results in human immune cells, we performed a longitudinal time-based assessment of cell viability and apoptosis in $CD4^+CD25^-$ T cells and CD4 deficient PBMCs undergoing immunomodulation with GAD65 +GC7+anti-DLL4 for seven days (Figures 6A, B and 7A). In Treg-deficient $CD4^+$ T cells, we did not observe any difference in the number of live, dead, or apoptotic cells in the treated and control groups until 48 h of treatment (Figure 6C). Post 96 hours, the dead cell count was significantly increased (P= 0.001) in the GAD65+GC7+anti-DLL4 treated group, wherein 25.1±3.4% of T cells were dead compared to 14.9±2.2% in the control group (Figure 6C). Similarly, the percentage of live T-cells decreased significantly (P=0.007) in the treated group on 7^{th} day (56.35±6.29%) compared with 72.1±4.04% in the control group (Figure 6C). To investigate the reason for the spike in dead cells in the treated group, we analyzed the phenotype of cells in both the treated and control groups on the 7^{th} day. Flow cytometry analysis revealed that 36.6% of live T cells in the treated group (Figure 6D and E) were newly plasticized Tregs owing to GAD65+GC7+anti-DLL4 treatment, expressing their suppressive phenotype and killing Teffs (Figure 6E). Hence, the suppression of Teffs was reflected by an increase in dead cell count. This was confirmed by the phenotype of live cells in the control group of autologous patient cells, in which most cells were non-regulatory (Figure 6D); hence, comparatively fewer dead cells were those undergoing physiological cell death.

In the CD4 deficient PBMCs, no changes were observed in live, dead, and apoptotic cells for up to 48 h in the GAD65 +GC7+anti-DLL4 treated and control groups (Figure 7B), however there was a significant sudden spike in the dead cell count in the GAD65+GC7+anti-DLL4 treated group (P=0.04), which continued until day 7 (P=0.0036) (Figure 7B). We again observed that the phenotype of live cells on the 7^{th} day is T regulatory (14.6±3.2%) in the treated group compared to 3.7±1.2% Tregs in the control group (Figure 7C and D). This implies that in the GAD65+GC7+anti-DLL4 treated group, there was a significant enrichment of Tregs (Figure 7C, P<0.03). These plasticized Tregs exhibit a functional suppressive phenotype, suppressing Teffs, which is manifested as an increase in dead cell count in the treated group beyond 96 h (Figure 7B–D) and no adverse effects of immunomodulatory treatment on the viability of immune cells. Hence, GAD65+GC7+anti-DLL4 did not exhibit cellular toxicity in the concentration range that plasticizes $CD4^+$ T cells or CD4 deficient PBMCs into Tregs.

Increased TGF-β Concentration in the Cell Culture Supernatant After GAD65+GC7 +anti-DLL4 Treatment

To support our findings, the concentration of TGF-β was quantified using the Human TGF beta1 ELISA Kit (Invitrogen). It was found to be higher in the supernatant of cells undergoing plasticization with GAD65+GC7+anti-DLL4 treatment (Figure 7E).

Discussion

For the treatment of autoimmune diseases, attempts to induce Tregs in vivo with low-dose IL-2 therapy or TGF-β have encountered significant limitations for use in clinical practice because of the pleiotropic role of these cytokines and the activation of cells other than Tregs (eosinophils, NK cells, and $CD8^+$ T cells).[40] In the case of TGF-β, a lower concentration, particularly in the presence of inflammatory cytokines such as IL-6 and IL-21, preferentially promotes the Th17 response and exacerbates Treg/Th17 imbalance.[41] Similarly, TNF blockers may paradoxically induce Th1/Th17 cells and dysregulate IFN response.[42] In T1D/LADA, therapeutic interventions have focused either on symptomatic treatment, mitigating islet β-cell stress, or polyclonal expansion of Tregs;[43] however, genuinely advantageous combination therapy should have a multipronged approach that simultaneously enriches Tregs, restrains CTLs, and decreases ER stress in islet β-cells.

The immunophenotype of T1D constitutes a reduced number of Tregs, which is too low to prevent perpetuating immune assault or unfit to confine the population of Teffs attacking the pancreatic islet β-cells.[3] In addition, aberrant plasticity of Treg cells is observed, with Treg cells expressing pro-inflammatory cytokines, acquiring T helper-like phenotypes, and displaying diminished function in most cases while maintaining $FOXP3^+$ expression levels.[44] We reported a significantly increased intermediate population of Tregs ($CD4^+CD25^-IFNg^+IL17^+FOXP3^+$) that maintained $FOXP3^+$ expression but also expressed proinflammatory cytokines in T1D/LADA patients (Figure 1B, C and Supplementary material S8). There is an increased frequency of $IFNg^+FOXP3^+$ Tregs in the periphery of patients with autoimmune diseases, such as T1D, multiple sclerosis, autoimmune hepatitis, and Sjogren syndrome, which display reduced suppressive capacities compared to Tregs from healthy age-matched subjects.[44] This pathological conversion of Tregs into Teff or Th17 type is not new; however, it is instrumental in visualizing $CD4^+CD25^-IFNg^+IL17^+FOXP3^+$ cells that are significantly increased in patients with recent-onset T1D/LADA (Figure 1B and Supplementary material S8). These $CD4^+IFNg^+IL17^+FOXP3^+$ intermediate cells are $CD25^-$ T cells (Figure 1C and Supplementary material S8), like EAE, wherein approximately 40% of the cells infiltrating the central nervous system are $CD4^+FOXP3^+CD25^-$ T cells. These transient Tregs play a role in promoting inflammation, as in multiple sclerosis and inflammatory bowel disease, where Tregs expressing $FOXP3^+IFNg^+$ are significantly abundant and convert to Teffs with subsequent loss of $FOXP3^+$ expression.[5,39,45,46] We hypothesized that this significantly expanded population of transient Tregs was previously characterized as unfit Tregs; however, therapeutic intervention could be reverted to functionally active Tregs (Figures 2B, F, 3G, 6D and 7C). This highly plastic intermediate subset originates from $CD4^+CD25^-$ T cells upon encountering an antigen, receiving extrathymic signals, or in a proinflammatory milieu. Thus, the inflammatory microenvironment is responsible for tipping these intermediate subsets towards the inflammatory phenotype. Contemporary TNF-α blockers augment the phosphorylation of $FOXP3^+$ and modulate aberrant transdifferentiation of Tregs in rheumatoid arthritis.[47] In the present study, $CD4^+CD25^-$ T cells from T1D/LADA patients showed an enriched population of intermediate Tregs ($CD4^+CD25^-IFNg^+IL17^+FOXP3^+$), which on treatment with GAD65+GC7+anti-DLL4 transdifferentiated into stable Tregs ($CD4^+CD25^+FOXP3^+$) (Figure 2B and F).

Furthermore, we observed the plasticization of Tregs from a pool of CD4 T cell-deficient PBMCs (Figure 3D–G). This cell pool mimicked the proinflammatory cytokine milieu typical of T1D/LADA (Supplementary material S9B), wherein APCs activated GAD65-specific $CD8^+$ T-cells. This illustrates that the combination treatment with GAD65 +GC7+anti-DLL4 can induce the differentiation of $CD8^+$ T cells into $CD4^+$ T cells and subsequent plasticization into $CD4^+CD25^+FOXP3^+$ Tregs under pro-inflammatory conditions (Figure 3G and Supplementary material S9 B). It is noteworthy that proinflammatory conditions hamper the induction of Tregs in vivo and hence limit the therapeutic potential of previously used immunomodulators, such as TGF-β.[32–34] Akamatsu et al[34] also reported that TGF-β-induced $FOXP3^+$ expression in Tregs was hampered under culture conditions containing inflammatory cytokines such as IL-12, IL-4, and IL-6. A key feature of our study was the induction and expansion of $CD25^+FOXP3^+$ T cells without IL-2 or TGF-β and withstanding the proinflammatory cytokine milieu (Supplementary material S9). Supported by our previous results from in vivo studies on eIF5a and Notch inhibition using GC7 and anti-DLL4, where we elucidated the intrathymic differentiation and enrichment of Tregs,[12] these in vitro results address the thymic-independent role of the adoption of Treg cell fate by $CD4^+$ and $CD8^+$ T cells. Although there are reports of plasticity of Tregs and Th17 cells, the characterization of $CD4^+CD25^-IFNg^+IL17^+FOXP3^+$ T cells in patients with T1D/LADA is unique, and the differentiation of functional Tregs from Treg-deficient $CD4^+$ T cells and CD4 T cell-deficient PBMCs sheds light on a new area of research in therapeutic interventions for autoimmune diseases.

Interconversion of immune cells (Th17, Tregs) is attributed to the inhibition of the polyamine and mTOR pathways and increased STAT5 phosphorylation independent of the thymus.[18,48] In vitro induction of FOXP3 by pharmacological inhibition of the CDK19 gene, leading to enhanced activation of STAT5, also emphasizes the role of the IL-2/STAT5 pathway in acquiring the Treg phenotype.[34] However, considering the web of signaling networks and their complexities, it is difficult to decipher the actual changeover of signals in real-time. Nevertheless, the newly plasticized Tregs displayed a functional phenotype and significantly suppressed autologous Teffs, indicating stable expression of the $CD25^+FOXP3^+$ suppressive phenotype (Figure 4B and C; 5B and C). Flow cytometry analysis revealed that they maintained their suppressive phenotype post-suppressive assay, negating interchangeability into Teff-Tregs (Figures 4C right upper

quarter, 5C right upper quarter). Moreover, plasticized Tregs from GAD65+GC7+anti-DLL4 had better proliferative potential than conventional CD3/CD28/137 stimulation (Figures 2D and, Figures 2F).

Hyp-eIF5a is overexpressed in $CD4^+$-activated T cells[49] in T1D[10,11] and exacerbates the diabetic phenotype.[8] GC7 inhibits hyp-eIF5a without changing its basal levels;[11] hence, it plays a restrictive role in translating a specific set of proteins. Moreover, depletion of eIF5a impairs translational elongation of only about 5% of mRNA;[6] therefore, depletion of eIF5a with GC7 may not produce any generalized adverse effects. This aligns with our results, wherein there were no adverse effects of GC7+anti-DLL4 on $CD4^+CD25^-$ T cells and CD4 T cell-deficient PBMCs (Figures 6 and 7). Oliverio et al[50] reported induction of autophagy in a cancer cell line within 24 h of treatment with GC7. However, our observation of immune cells with GC7 (100μM/mL) did not reveal any changes in the percentage of apoptotic and live/dead cells for up to 48 h, suggesting that GC7 at the given concentration does not induce autophagy (Figures 6C and 7B) in peripheral immune cells. The transient nature of autophagy further supports this because it is a short-lived cellular adaptation of cells to stress, evident within hours, and cannot be sustained for a long time. The phenotype of cells on the 7^{th} day (Figure 7C) and TGF-β concentration in the cell culture supernatant (Figure 7E) clearly revealed that Tregs exerted their suppressive phenotype on Teffs, manifested as an increase in dead cells after 96 h. This study is conducted with a small cohort (n=7 for both healthy individuals and T1D patients), but it offers a robust proof-of-concept for the generation of Tregs in humans, paving the way for large-scale validation. Moreover, all experiments were replicated with sufficient technical replicates to ensure reliability. Thus, the current experiments, which revealed no adverse effects on cell viability with immunomodulatory treatment, and with previous studies in a humanized mouse model of T1D[10–12] and DHPS+/- mice,[6] that did not lead to any significant suppression of cellular proliferation and maintained normal growth, demonstrate a reassuring safety profile and strategic use of this treatment approach.

Conclusion

Antigen-specific Treg enrichment and depletion of CTLs are the key targets of the T1D/LADA cure. Our findings represent the culmination and synthesis of previous findings on the use of GC7 in human and mouse islets and spontaneous humanized T1D mice, anti-DLL4 inhibition in NOD mice, and spontaneous humanized T1D mice. Our study identified a unique population of $CD4^+CD25^-IFNg^+IL17^+FOXP3^+$ T cells in T1D/LADA patients that successfully reverted to functionally active Tregs, thereby suppressing diabetogenic Teffs. Most importantly, this approach could induce plasticity in a proinflammatory microenvironment without adversely affecting immune cells. The addition of findings from human in vitro studies serves as a definitive endpoint in exploring immunomodulatory treatment with GC7 +anti-DLL4, which addresses the immunological cascade of events in T1D, as well as metabolic/pathophysiological inflammation-mediated ER stress, and facilitates the design of innovative immunotherapy for LADA/T1D and other autoimmune diseases. This therapeutic strategy is not only pivotal for generating Tregs to treat T1D but also holds potential for supporting islet transplantation and serving as a complementary method to enhance the efficacy of adoptive cell therapy. It would be interesting to decipher the sequential events and signaling pathways involved in Treg differentiation in CD4 T cell-deficient PBMCs. We speculate that in the GAD65+GC7+anti-DLL4 treated group, $CD8^+$ T cells first dedifferentiated into double-negative/double-positive T cells and then redifferentiated into specific $CD4^+CD25^+$ T cells expressing FOXP3. These findings may be further validated by RNA-seq analysis of cells at different stages of plasticization.

Abbreviations

APCs, Antigen-presenting cells; BMI, Body mass index; CFSE, Carboxyfluorescein Diacetate, Succinimidyl Ester; CTL, Cytotoxic T lymphocytes; DHS, Deoxyhypusine synthase; DLL4, Delta like ligand 4; EAE, Experimental autoimmune encephalitis; eIF5a, eukaryotic initiation factor 5a; ER, Endoplasmic reticulum; GAD65, Glutamic acid decarboxylase 65-kilodalton isoform; GC7, N1-Guanyl-1,7-diaminoheptane; IFNg, Interferon-gamma; JAK3, Tyrosine-protein kinase JAK3; LADA, Latent onset of autoimmune diabetes; mTOR, Mechanistic target of Rapamycin; PBMCs, Peripheral blood mononuclear cells; rhGAD65, recombinant human GAD65; ROR-γt, Retinoic acid-related orphan receptor ROR-γt; STAT5, Signal transducer and activator of transcription 5; T1D, Type 1 diabetes; Teff, Effector T cell; TGF-β, Transforming growth factor β; Th, T helper; Treg, Regulatory T cell; Tresp, Responder T cell.

Data Sharing Statement

The original contributions of this study are included in the manuscript, as well as supplementary data. Further research can be directed to the corresponding author, Shahnawaz Imam Shahnawaz.imam@utoledo.edu.

Ethics Approval and Consent to Participate

Healthy adults and patients with T1D/LADA signed informed consent forms and were enrolled in this study, which was rigorously approved by the Institutional Review Board of the University of Toledo (IRB). Ethical approval ensured that the research was conducted with the highest standards of integrity and respect for the participants. The research adhered to the principles stated in the Declaration of Helsinki.

Acknowledgments

This work was supported by the University of Toledo start-up funding and a Pilot and Feasibility Grant from the Michigan Diabetes Research Center (NIH Grant P30-DK020572) received by the SI. The authors thank the Flow Cytometry Core of the University of Toledo, the University of Toledo Medical Center, and the associated hospital staff, volunteers, and patients for their kind consent to donate the blood samples.

Author Contributions

All authors made a significant contribution to the work reported, whether that is in the conception, study design, execution, acquisition of data, analysis and interpretation, or in all these areas; took part in drafting, revising or critically reviewing the article; gave final approval of the version to be published; have agreed on the journal to which the article has been submitted; and agree to be accountable for all aspects of the work.

Disclosure

Immunomodulators and their uses have been patented (United States Provisional Patent Application No. 63389391: Synergistic Inhibition of eIF5A and Notch Signaling. University of Toledo, Office of Technology Transfer, year 2022, primary inventors S Imam, JC Jaume; https://patents.google.com/patent/US20240148789A1/en). Another CIP application, titled 'Synergistic Inhibition of eIF5A and Notch Signaling in intermediate Tregs (US Patent App. US18/670,112, 2024; https://patents.google.com/patent/US20240307532A1, primary inventors S Imam, Shafiya Imtiaz Rafiqi) has been filed. The authors declare that they have no other conflicts of interest in this work.

References

1. Papadopoulou G, Xanthou G. Metabolic rewiring: a new master of Th17 cell plasticity and heterogeneity. *FEBS J*. 2022;289(9):2448–2466. doi:10.1111/febs.15853
2. Feng T, Cao AT, Weaver CT, Elson CO, Cong Y. Interleukin-12 Converts Foxp3+ Regulatory T Cells to Interferon–γ-Producing Foxp3+ T Cells That Inhibit Colitis. *Gastroenterology*. 2011;140(7):2031–2043. doi:10.1053/j.gastro.2011.03.009
3. Hull CM, Peakman M, Tree TIM. Regulatory T cell dysfunction in type 1 diabetes: what's broken and how can we fix it? *Diabetologia*. 2017;60 (10):1839–1850. doi:10.1007/s00125-017-4377-1
4. Esposito M, Ruffini F, Bergami A, et al. IL-17– and IFN-γ–Secreting Foxp3+ T Cells Infiltrate the Target Tissue in Experimental Autoimmunity. *J Immunol*. 2010;185(12):7467–7473. doi:10.4049/jimmunol.1001519
5. Komatsu N, Okamoto K, Sawa S, et al. Pathogenic conversion of Foxp3+ T cells into TH17 cells in autoimmune arthritis. *Nat Med*. 2014;20(1):62–68. doi:10.1038/nm.3432
6. Templin AT, Maier B, Nishiki Y, Tersey SA, Mirmira RG. Deoxyhypusine synthase haploinsufficiency attenuates acute cytokine signaling. *Cell Cycle*. 2011;10(7):1043–1049. doi:10.4161/cc.10.7.15206
7. Mastracci TL, Colvin SC, Padgett LR, Mirmira RG. Hypusinated eIF5A is expressed in the pancreas and spleen of individuals with type 1 and type 2 diabetes. Ciccacci C, editor. *PLoS One*. 2020;15(3):e0230627. doi:10.1371/journal.pone.0230627
8. Kulkarni A, Anderson CM, Mirmira RG, Tersey SA. Role of Polyamines and Hypusine in β Cells and Diabetes Pathogenesis. *Metabolites*. 2022;12 (4):344. doi:10.3390/metabo12040344
9. Colvin SC, Maier B, Morris D, et al. Deoxyhypusine synthase promotes differentiation and proliferation of T helper type 1 (Th1) cells in autoimmune diabetes. *J Biol Chem*. 2013;288(51):36226–36235. doi:10.1074/jbc.M113.473942
10. Imam S, Mirmira RG, Jaume JC. Eukaryotic translation initiation factor 5A inhibition alters physiopathology and immune responses in a "humanized" transgenic mouse model of type 1 diabetes. *Am J Physiol Endocrinol Metab*. 2014;306(7):E791–8. doi:10.1152/ajpendo.00537.2013
11. Imam S, Prathibha R, Dar P, et al. eIF5A inhibition influences T cell dynamics in the pancreatic microenvironment of the humanized mouse model of Type 1 Diabetes. *Sci Rep*. 2019;9(1):1533. doi:10.1038/s41598-018-38341-5

12. Imam S, Dar P, Aziz SW, et al. Immune Cell Plasticity Allows for Resetting of Phenotype From Effector to Regulator With Combined Inhibition of Notch/eIF5A Pathways. *Front Cell Dev Biol*. 2021;9:777805. doi:10.3389/fcell.2021.777805
13. Maier B, Ogihara T, Trace AP, et al. The unique hypusine modification of eIF5A promotes islet β cell inflammation and dysfunction in mice. *J Clin Invest*. 2010;120(6):2156–2170. doi:10.1172/JCI38924
14. Cho OH, Shin HM, Miele L, et al. Notch Regulates Cytolytic Effector Function in CD8+ T Cells. *J Immunol*. 2009;182(6):3380–3389. doi:10.4049/jimmunol.0802598
15. Kuijk LM, Verstege MI, Rekers NV, et al. Notch controls generation and function of human effector CD8+ T cells. *Blood*. 2013;121(14):2638–2646. doi:10.1182/blood-2012-07-442962
16. Bassil R, Zhu B, Lahoud Y, et al. Notch Ligand Delta-Like 4 Blockade Alleviates Experimental Autoimmune Encephalomyelitis by Promoting Regulatory T Cell Development. *J Immunol*. 2011;187(5):2322–2328. doi:10.4049/jimmunol.1100725
17. Billiard F, Lobry C, Darrasse-Jèze G, et al. Dll4–Notch signaling in Flt3-independent dendritic cell development and autoimmunity in mice. *J Exp Med*. 2012;209(5):1011–1028. doi:10.1084/jem.20111615
18. Magee CN, Murakami N, Borges TJ, et al. Notch-1 Inhibition Promotes Immune Regulation in Transplantation Via Regulatory T Cell–Dependent Mechanisms. *Circulation*. 2019;140(10):846–863. doi:10.1161/CIRCULATIONAHA.119.040563
19. Chiplunkar SV, Gogoi D. The multifaceted role of Notch signal in regulating T cell fate. *Immunol Lett*. 2019;206:59–64. doi:10.1016/j.imlet.2019.01.004
20. Regulatory T cells | t cell isolation | in vitro suppression | miltenyi Biotec | USA. Available from: https://www.miltenyibiotec.com/US-en/applications/all-protocols/human-cd4-cd25-regulatory-t-cell-isolation-in-vitro-suppression-assay-and-analysis. Accessed February 25, 2025.
21. Imam S, Dar P, Paparodis R, et al. Nature of coexisting thyroid autoimmune disease determines success or failure of tumor immunity in thyroid cancer. *J Immunother Cancer*. 2019;7(1):3. doi:10.1186/s40425-018-0483-y
22. Imam S, Paparodis RD, Rafiqi SI, et al. Thyroid Cancer Screening Using Tumor-Associated DN T Cells as Immunogenomic Markers. *Front Oncol*. 2022;12:891002. doi:10.3389/fonc.2022.891002
23. Imam S, Paparodis R, Sharma D, Jaume JC. Lymphocytic profiling in thyroid cancer provides clues for failure of tumor immunity. *Endocr Relat Cancer*. 2014;21(3):505–516. doi:10.1530/ERC-13-0436
24. Imam S, Rafiqi SI. Synergistic Inhibition of eIF5A and Notch Signaling in Intermediate Tregs. US Patent App. US18/670,112, 2024, https://patents.google.com/patent/US20240307532A1. Accessed February 25, 2025.
25. Voo KS, Wang YH, Santori FR, et al. Identification of IL-17-producing FOXP3^{+} regulatory T cells in humans. *Proc Natl Acad Sci*. 2009;106(12):4793–4798. doi:10.1073/pnas.0900408106
26. Horwitz DA. Identity of mysterious CD4+CD25-Foxp3+cells in systemic lupus erythematosus. *Arthritis Res Ther*. 2010;12(1):1–3. doi:10.1186/ar2894
27. Yang XO, Nurieva R, Martinez GJ, et al. Molecular Antagonism and Plasticity of Regulatory and Inflammatory T Cell Programs. *Immunity*. 2008;29(1):44–56. doi:10.1016/j.immuni.2008.05.007
28. Serr I, Drost F, Schubert B, Daniel C. Antigen-Specific Treg Therapy in Type 1 Diabetes – challenges and Opportunities. *Front Immunol*. 2021;12:712870. doi:10.3389/fimmu.2021.712870
29. Ma X, Cao L, Raneri M, et al. Human HLA-DR^{+}CD27^{+} regulatory T cells show enhanced antigen-specific suppressive function. *JCI Insight*. 2023;8(23). doi:10.1172/jci.insight.162978
30. Sakaguchi S, Kawakami R, Mikami N. Treg-based immunotherapy for antigen-specific immune suppression and stable tolerance induction: a perspective. *Immunother Adv*. 2023;3(1):ltad007. doi:10.1093/immadv/ltad007
31. Zloza A, Sullivan YB, Connick E, Landay AL, Al-Harthi L. CD8+ T cells that express CD4 on their surface (CD4dimCD8bright T cells) recognize an antigen-specific target, are detected in vivo, and can be productively infected by T-tropic HIV. *Blood*. 2003;102(6):2156–2164. doi:10.1182/blood-2002-07-1972
32. Shevach EM, Thornton AM. tTregs, pTregs, and iTregs: similarities and differences. *Immunol Rev*. 2014;259(1):88–102. doi:10.1111/imr.12160
33. Xu L, Kitani A, Strober W. Molecular mechanisms regulating TGF-β-induced Foxp3 expression. *Mucosal Immunol*. 2010;3(3):230–238. doi:10.1038/mi.2010.7
34. Akamatsu M, Mikami N, Ohkura N, et al. Conversion of antigen-specific effector/memory T cells into Foxp3-expressing Treg cells by inhibition of CDK8/19. *Sci Immunol*. 2019;4(40):eaaw2707. doi:10.1126/sciimmunol.aaw2707
35. Wang J, Ioan-Facsinay A, Van der voort EI, Huizinga TW, Toes RE. Transient expression of FOXP3 in human activated nonregulatory CD4+ T cells. *Eur J Immunol*. 2007;37(1):129–138. doi:10.1002/eji.200636435
36. Gavin MA, Torgerson TR, Houston E, et al. Single-cell analysis of normal and FOXP3-mutant human T cells: FOXP3 expression without regulatory T cell development. *Proc Natl Acad Sci*. 2006;103(17):6659–6664. doi:10.1073/pnas.0509484103
37. Tran DQ, Ramsey H, Shevach EM. Induction of FOXP3 expression in naive human CD4+FOXP3− T cells by T-cell receptor stimulation is transforming growth factor-β–dependent but does not confer a regulatory phenotype. *Blood*. 2007;110(8):2983–2990. doi:10.1182/blood-2007-06-094656
38. Miyao T, Floess S, Setoguchi R, et al. Plasticity of Foxp3+ T cells reflects promiscuous Foxp3 expression in conventional t cells but not reprogramming of regulatory T cells. *Immunity*. 2012;36(2):262–275. doi:10.1016/j.immuni.2011.12.012
39. Kitz A, Dominguez-Villar M. Molecular mechanisms underlying Th1-like Treg generation and function. *Cell mol Life Sci*. 2017;74(22):4059–4075. doi:10.1007/s00018-017-2569-y
40. Ghobadinezhad F, Ebrahimi N, Mozaffari F, et al. The emerging role of regulatory cell-based therapy in autoimmune disease. *Front Immunol*. 2022;13:1075813. doi:10.3389/fimmu.2022.1075813
41. Li MO, Flavell RA. TGF-beta: a master of all T cell trades. *Cell*. 2008;134(3):392–404. doi:10.1016/j.cell.2008.07.025
42. Jung SM, Kim WU. Targeted Immunotherapy for Autoimmune Disease. *Immune Netw*. 2022;22(1):e9. doi:10.4110/in.2022.22.e9
43. Von scholten BJ, Kreiner FF, Gough SCL, von Herrath M. Current and future therapies for type 1 diabetes. *Diabetologia*. 2021;64(5):1037–1048. doi:10.1007/s00125-021-05398-3
44. Dominguez-Villar M, Hafler DA. Regulatory T cells in autoimmune disease. *Nat Immunol*. 2018;19(7):665–673. doi:10.1038/s41590-018-0120-4
45. Jiang Z, Zhu H, Wang P, et al. Different subpopulations of regulatory T cells in human autoimmune disease, transplantation, and tumor immunity. *MedComm*. 2022;3(2):e137. doi:10.1002/mco2.137

46. Rajendiran A, Tenbrock K. Regulatory T cell function in autoimmune disease. *J Trans Autoimmun*. 2021;4:100130. doi:10.1016/j.jtauto.2021.100130
47. Alunno A, Bistoni O, Gerli R. Beware of wolves in sheep's clothing: immune cell plasticity and instability in health and disease. *Ann Rheum Dis*. 2022;81(7):e129–e129. doi:10.1136/annrheumdis-2020-218094
48. Shi H, Chi H. Polyamine: a metabolic compass for T helper cell fate direction. *Cell*. 2021;184(16):4109–4112. doi:10.1016/j.cell.2021.07.012
49. Puleston DJ, Baixauli F, Sanin DE, et al. Polyamine metabolism is a central determinant of helper T cell lineage fidelity. *Cell*. 2021;184(16):4186–4202.e20. doi:10.1016/j.cell.2021.06.007
50. Oliverio S, Corazzari M, Sestito C, Piredda L, Ippolito G, Piacentini M. The spermidine analogue GC7 (N1-guanyl-1,7-diamineoheptane) induces autophagy through a mechanism not involving the hypusination of eIF5A. *Amino Acids*. 2014;46(12):2767–2776. doi:10.1007/s00726-014-1821-0